PYHIN protein IFI207 regulates cytokine transcription and IRF7 and contributes to the establishment of K. pneumoniae infection

Baran, M., Feriotti, C., McGinley, A., Carlile, S. R., Jiang, Z., Calderon-Gonzalez, R., Dumigan, A., Sá-Pessoa, J., Sutton, C. E., Kearney, J., McLoughlin, R. M., Mills, K. H. G., Fitzgerald, K. A., Bengeochea, J. A., & Bowie, A. G. (2023). PYHIN protein IFI207 regulates cytokine transcription and IRF7 and contributes to the establishment of K. pneumoniae infection. *Cell Reports*, *42*(4), Article 112341. Advance online publication. https://doi.org/10.1016/j.celrep.2023.112341

Published in:
Cell Reports

Document Version:
Publisher's PDF, also known as Version of record

Cell Reports

Article

PYHIN protein IFI207 regulates cytokine transcription and IRF7 and contributes to the establishment of *K. pneumoniae* infection

Graphical abstract

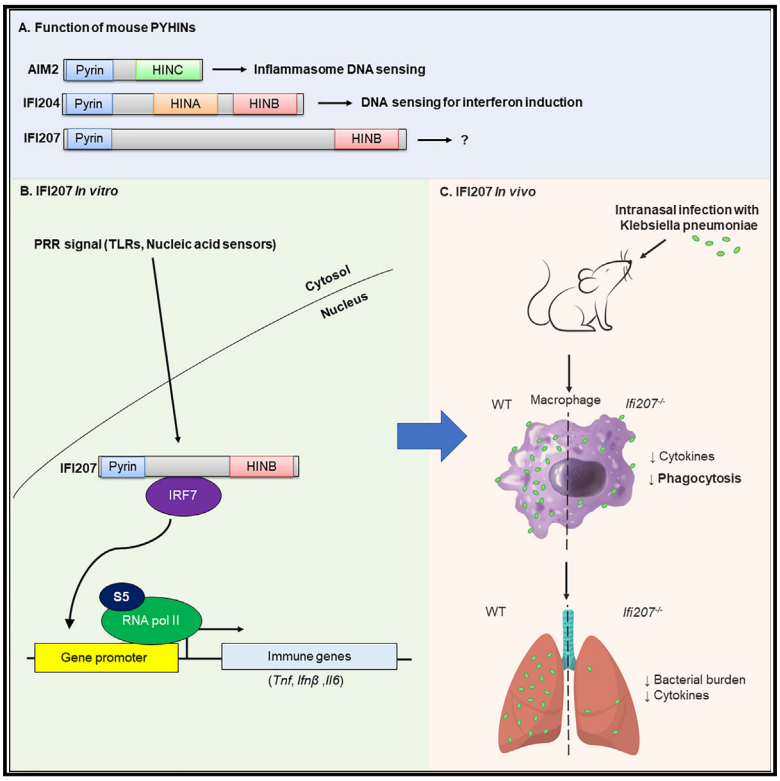

Highlights

- PYHIN protein IFI207 has roles in innate immunity distinct from AIM2 and IFI204
- IFI207 positively regulates cytokine gene induction in macrophages from the nucleus
- IFI207 engages with IRF7 and co-localizes with active RNA polymerase II
- *Klebsiella* requires IFI207 for macrophage entry and to establish a lung infection

Authors

Marcin Baran, Claudia Feriotti, Aoife McGinley, ..., Katherine A. Fitzgerald, Jose A. Bengeochea, Andrew G. Bowie

Correspondence

agbowie@tcd.ie

In brief

PYHIN proteins are implicated in innate immune responses to pathogens, but many remain uncharacterized. Baran et al. show that mouse PYHIN protein IFI207 positively regulates IRF7 and cytokine gene induction in macrophages while also being required for *Klebsiella* to enter macrophages and to establish a lung infection.

Baran et al., 2023, Cell Reports *42*, 112341
April 25, 2023
https://doi.org/10.1016/j.celrep.2023.112341

CellPress

Cell Reports

CellPress
OPEN ACCESS

Article

PYHIN protein IFI207 regulates cytokine transcription and IRF7 and contributes to the establishment of *K. pneumoniae* infection

Marcin Baran,[1] Claudia Feriotti,[2] Aoife McGinley,[1] Simon R. Carlile,[1] Zhaozhao Jiang,[3] Ricardo Calderon-Gonzalez,[2] Amy Dumigan,[2] Joana Sá-Pessoa,[2] Caroline E. Sutton,[1] Jay Kearney,[1] Rachel M. McLoughlin,[1] Kingston H.G. Mills,[1] Katherine A. Fitzgerald,[3] Jose A. Bengeochea,[2] and Andrew G. Bowie[1,4,*]

[1]School of Biochemistry and Immunology, Trinity Biomedical Sciences Institute, Trinity College Dublin, Dublin 2 Dublin, Ireland
[2]Wellcome-Wolfson Institute for Experimental Medicine, School of Medicine, Dentistry and Biomedical Sciences, Queens University Belfast, 97 Lisburn Road, Belfast, UK
[3]Division of Innate Immunity, University of Massachusetts Chan Medical School, Worcester, MA, USA
[4]Lead contact
*Correspondence: agbowie@tcd.ie
https://doi.org/10.1016/j.celrep.2023.112341

SUMMARY

PYHIN proteins AIM2 and IFI204 sense pathogen DNA, while other PYHINs have been shown to regulate host gene expression through as-yet unclear mechanisms. We characterize mouse PYHIN IFI207, which we find is not involved in DNA sensing but rather is required for cytokine promoter induction in macrophages. IFI207 co-localizes with both active RNA polymerase II (RNA Pol II) and IRF7 in the nucleus and enhances IRF7-dependent gene promoter induction. Generation of *Ifi207*$^{-/-}$ mice shows no role for IFI207 in autoimmunity. Rather, IFI207 is required for the establishment of a *Klebsiella pneumoniae* lung infection and for *Klebsiella* macrophage phagocytosis. These insights into IFI207 function illustrate that PYHINs can have distinct roles in innate immunity independent of DNA sensing and highlight the need to better characterize the whole mouse locus, one gene at a time.

INTRODUCTION

PYHIN proteins are characterized by the presence of an N-terminal Pyrin domain (PYD) and one or two C-terminal DNA-binding HIN domains. There are 5 PYHIN genes in humans (*IFI16*, *MNDA*, *PYHIN1/IFIX*, *AIM2*, and *POP3*) and 13 in mouse (*Ifi202*, *Ifi203*, *Ifi204*, *Ifi205*, *Ifi206*, *Ifi207*, *Ifi208*, *Ifi209*, *Ifi210/Aim2*, *Ifi211*, *Ifi212*, *Ifi213*, and *Ifi214*).[1–3] Initially, PYHINs were implicated in cell cycle regulation, cell proliferation, modulation of cell survival, and cell differentiation[4,5] but are now known to also function in immune responses to pathogens. Thus some PYHINs act as pattern-recognition receptors (PRRs), sensing intracellular double-stranded DNA (dsDNA) for type I interferon (IFN) production (IFI16, IFI204)[6] or for inflammasome activation (AIM2, IFI16).[7,8] IFI16 is also a restriction factor for some viruses[9,10] since it can directly bind to viral genomes via one of its HIN domains, as well as sequestering proteins needed for viral transcription via its PYD.[11,12]

PYHINs are located both in the cytosol (AIM2, POP3, Ifi202, Ifi206) and the nucleus (IFI16, IFI204, Ifi205, PYHIN1/IFIX, myeloid cell nuclear differentiation antigen [MNDA]).[3,6,7,13,14] The nuclear PYHINs IFI16, PYHIN1, MNDA and IFI205 can regulate transcription of certain immune genes by largely undefined mechanisms.[14–17] Increased expression of PYHINs and/or PYHIN autoantibodies are seen in autoimmune disorders such as systemic lupus erythematosus (SLE),[18,19] psoriasis,[20] rheumatoid arthritis (RA),[21] and inflammatory bowel disease (IBD).[22] Additionally, AIM2 drives the development of experimental autoimmune encephalomyelitis (EAE), a mouse model of multiple sclerosis (MS), due to a role in regulation of regulatory T (Treg) cell fate and activation of microglia.[23,24]

Studies to date therefore show that PYHINs regulate immune responses through diverse mechanisms including direct pathogen detection and modulation of host gene induction. However, apart from AIM2, the function of most of the mouse PYHINs has not been explored, while mechanistic insights into how PYHINs function at the molecular level are still lacking. Since we found that mouse PYHIN IFI207 was expressed in immune cells and upregulated in response to PRR stimulation, here we characterized its function. We reveal that unlike IFI204, IFI207 is not involved in DNA sensing but rather is required for transcriptional regulation of cytokines including *Tnf* in macrophages. We identify the protein domains required for IFI207-dependent transcriptional regulation and show that IFI207 co-localized both with active RNA polymerase II (RNA Pol II) and with the transcription factor IRF7 in the nucleus. By generating an *Ifi207*$^{-/-}$ mouse, we show that unlike AIM2, IFI207 has no role in autoimmune disease (EAE) but is required by *Klebsiella pneumoniae* to establish a lung infection. Thus, our findings on IFI207 give mechanistic insights into how PYHINs regulate innate immunity.

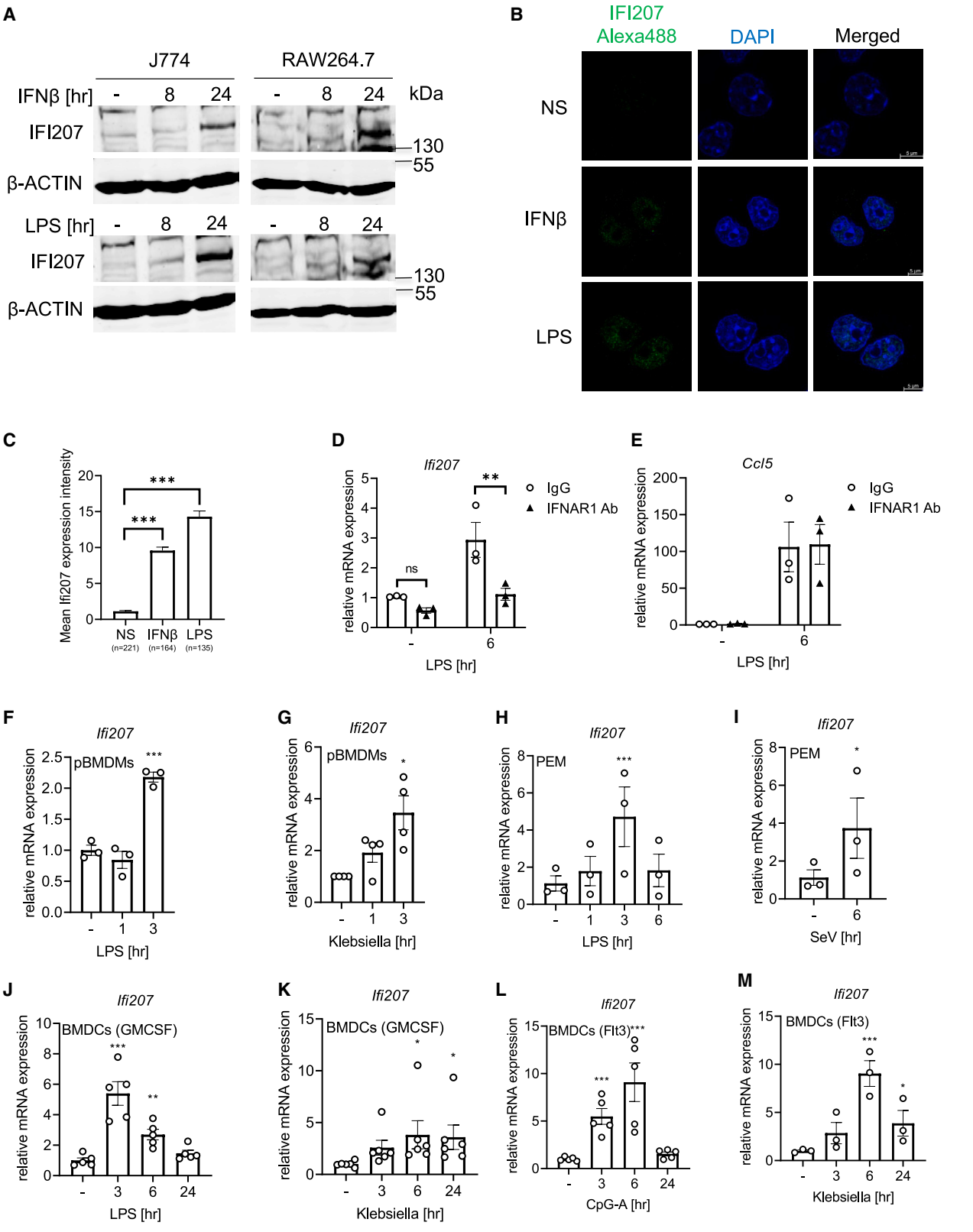

(legend on next page)

RESULTS

IFI207 is regulated by immune stimulants in macrophages

To examine PYHIN expression in immune cell populations, splenocytes from C57BL/6 mice were sorted by fluorescence-activated cell sorting (FACS) into cell populations characterized by the surface expression of either F4/80$^+$ (macrophages), CD11c$^+$ (dendritic cells [DCs]), TCRβ^+ (T cells), or CD19$^+$ (B cells) markers. *Ifi203*, *Ifi206*, *Ifi208*, *Ifi209*, *AIM2*/*Ifi210*, *Ifi212*, *Ifi213*, and *Ifi214* mRNA expression was evenly distributed between different cell types and showed similar expression to mixed splenocytes (Figures S1A, S1D, and S1F–S1K). Due to its sequence similarity to other family members, we were unable to design primers specifically detecting expression of *Ifi211*. Additionally, *Ifi202* mRNA expression in our samples was undetectable, consistent with a previous study of C57BL/6 splenocytes.[2] Of note, *Ifi204*, *Ifi205*, and *Ifi207*, in contrast to other family members, showed higher mRNA expression in F4/80$^+$ macrophages, while *Ifi205* was also expressed at a higher level in CD11c$^+$ DCs (Figures S1B, S1C, and S1E). While the role of IFI204 and IFI205 in macrophages has been previously studied,[6,14,25] nothing was known about IFI207's function, and we therefore focused on characterizing this PYHIN.

To study IFI207 protein expression in macrophages, we generated and validated a rabbit anti-IFI207 peptide antibody (Figure S1L). Previously, murine PYHIN expression was shown to be induced by type I IFNs,[3] and here, although we could not detect IFI207 in unstimulated cells, treatment of either RAW264.7 or J774 macrophage cell lines with IFNβ induced detectable IFI207 protein expression, as did treatment with lipopolysaccharide (LPS) (Figure 1A). The specificity of the detected band was further confirmed later in bone marrow-derived macrophages (BMDMs) from *Ifi207*$^{-/-}$ mice (Figures 3C and 3D).

We next assessed IFI207 expression by confocal microscopy (Figure 1B). Unstimulated immortalized BMDMs (iBMDMs) showed only very faint staining for IFI207, which was increased following stimulation with both IFNβ and LPS (Figure 1B), in correlation with the observed induction of IFI207 protein (Figure 1A). In all cases, the staining was almost exclusively localized within the nucleus. At the same time, similar staining was not detected with the immunoglobulin G (IgG) control antibody (Figure S5D). Figure 1C quantifies the increased nuclear staining of IFI207 after IFNβ or LPS stimulation. Thus, IFI207 is localized in the nucleus. Further, LPS-mediated *Ifi207* induction was due to LPS-produced type I IFN since incubating macrophages with an IFN-α/β receptor (IFNAR)-blocking antibody completely abrogated LPS-stimulated *Ifi207* mRNA induction (Figure 1D) compared with a lack of effect on LPS-stimulated *Ccl5* mRNA induction (Figure 1E). The IFNAR-blocking antibody also showed a small, but not significant, reduction of basal *Ifi207* mRNA expression (Figure 1D), suggesting that tonic IFNβ might have a role in maintaining the IFI207 expression in these cells.

Next, we examined IFI207 induction in primary myeloid cells in response to both PRR stimulation and pathogen infection. We stimulated primary BMDMs (Figures 1F and 1G), peritoneal macrophages (PEMs; Figures 1H and 1I), granulocyte macrophage colony-stimulating factor (GM-CSF)-differentiated cDC2 BMDCs (Figures 1J and 1K) and Flt3-differentiated cDC1 BMDCs (Figure 1L, 1M) derived from wild-type (WT) C57BL/6 mice with LPS or CpG-A or infected them with *K. pneumoniae* strain CIP52.145 (hereafter Kp52145) or Sendai virus (SeV). All treatments resulted in a significant increase of IFI207 mRNA expression in all tested cells, with expression peaking between 3 and 6 h post-stimulation (Figures 1F–1M). Such early induction of gene expression in both macrophages and DCs in response to pathogen-associated molecular patterns (PAMPs) and pathogens is often observed among genes involved in the innate immune response, which encouraged us to further explore IFI207's function.

IFI207 is required for *Tnf* induction after PRR stimulation

Many of the mouse *PYHIN* genes likely originated as a result of duplication, domain swapping, and other gene rearrangement events resulting from evolutionary pressures.[2,3] A phylogenetic analysis of mouse PYHIN genes showed that *Ifi207* is most closely related to *Ifi204* (Figure S2A). IFI207 is the largest mouse PYHIN protein (978 aa), and similar to other family members, it contains an N-terminal PYD and a C-terminal HIN200 domain, specifically an HINB domain (Figure 2A). The amino acid sequences of IFI207 and IFI204 Pyrin and HINB domains were 85% similar (with only 11 aa differing between them) and 92% similar (13 aa difference), respectively (Figures 2A, S2B, and S2C). Key amino acids previously identified within the HINB

Figure 1. Regulation of IFI207 expression in myeloid cells

(A) Immunoblot analysis of IFI207 expression in RAW264.7 and J774 macrophages stimulated with 1,000 U/mL IFNβ or 10 ng/mL LPS. Representative of 3 independent experiments.

(B and C) Confocal microscopy of immortalized BMDMs (iBMDMs) stimulated with 1,000 U/mL IFNβ or 100 ng/mL LPS for 24 h. IFI207 expression shown in green, while nuclei are stained blue with DAPI (B). Presented field of view (FOV) is representative of multiple FOVs taken from 2 independent experiments. IFI207 expression within the nucleus, as defined by DAPI staining, was quantified using ImageJ software, and data are presented as mean ± SEM of IFI207 expression intensity from 221 unstimulated cells (NS) and 164 IFNβ- and 135 LPS-treated cells (C). Statistical analysis was performed using two-tailed unpaired Student's t test.

(D and E) RAW264.7 macrophages were incubated overnight with 5 μg/mL either IFNAR1-blocking antibody or a non-specific IgG. Cells were then stimulated with 100 ng/mL LPS for 6 h, and expression of *Ifi207* (D) or *Ccl5* (E) mRNA was detected by qPCR. Data are the mean ± SEM of three independent experiments, each performed in triplicate.

(F–M) *Ifi207* mRNA expression in BMDMs (F and G), peritoneal macrophages (PEMs) (H and I), and GM-CSF- (J and K) or Flt3- (L and M) differentiated BMDCs infected with 100 MOI *K. pneumoniae* (G, K, and M) or SeV (I) or stimulated with 100 ng/mL LPS (F, H, and J) or 1 μg/mL CpG-A (L). Data shown are mean ± SEM of 3–6 mice. Statistical analysis in (D)–(M) was performed using two-way ANOVA.

For all panels, *p < 0.05, **p < 0.01, and ***p < 0.001 indicate significance between compared samples.

See also Figure S1.

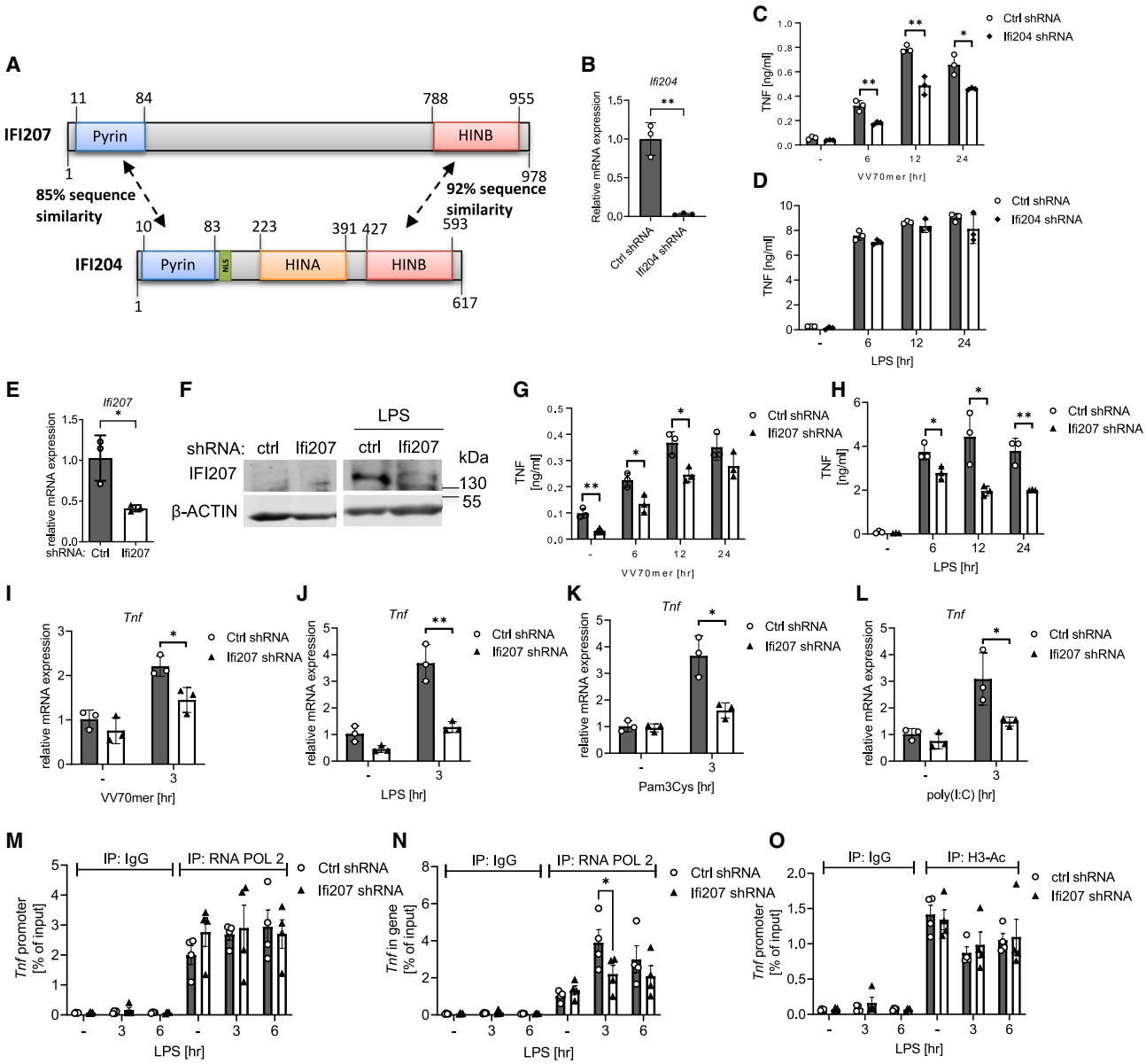

Figure 2. IFI207 is required for *Tnf* induction after PRR stimulation

(A) Schematic of IFI207 and IFI204 proteins indicating amino acid sequence similarity between the Pyrin and HINB domains of IFI207 and IFI204.

(B–D) RAW264.7 cells stably expressing control (Ctrl shRNA) or *Ifi204*-targeting shRNA (Ifi204 shRNA) were transfected with 1 μg/mL VV70mer (C) or stimulated with 100 ng/mL LPS (D). Knockdown of *Ifi204* mRNA was confirmed by qPCR (B), and TNF secretion was measured by ELISA (C and D).

(E and F) Knockdown of *Ifi207* in shRNA-expressing RAW264.7 cells was confirmed by qPCR (E) and western blot (F).

(G–L) RAW264.7 cells expressing either control (Ctrl) shRNA or shRNA targeting the 3′ UTR of *Ifi207* (Ifi207 shRNA) were transfected with 1 μg/mL VV70mer (G) or stimulated with 100 ng/mL LPS (H). TNF secretion was measured by ELISA (G and H). (I–L) As in (G) except cells were transfected with 1 μg/mL VV70mer (I) or 5 μg/mL poly I:C (L) or stimulated with 100 ng/mL LPS (J) or 1 μg/mL Pam3Cys (K). *Tnf* mRNA expression detected by qPCR. Data in (B)–(L) are representative of three independent experiments. qRT-PCR (B, E, and I–L) and ELISA (C, D, G, and H) data shown are mean ± SD of triplicate samples. Statistical analysis was performed using two-tailed unpaired Student's t test.

(M–O) J774 cells expressing control shRNA (Ctrl) or *Ifi207* shRNA were stimulated with 100 ng/mL LPS. Binding of RNA Pol II to *Tnf* promoter (M) or within the last exon of *Tnf* gene (N) as well as histone H3 acetylation of *Tnf* promoter (O) were detected by chromatin immunoprecipitation (ChIP) and calculated as the percentage of input. Non-specific IgG was used as negative control. Data shown are the mean ± SEM of 4 independent experiments. Statistical analysis was performed using two-way ANOVA.

For all panels, *$p < 0.05$ and **$p < 0.01$ indicate significance between compared samples.

See also Figures S2 and S3.

domain of IFI204 as important for mediating dsDNA binding were also conserved in IFI207 (Figure S2C).[26]

The close similarity of IFI207 and IFI204 (Figure 2A) suggested that IFI207 may function similarly to IFI204, as a DNA sensor. We therefore used short hairpin RNA (shRNA) targeting either *Ifi204* or *Ifi207* to compare their roles in DNA-dependent and DNA-independent signaling in macrophages. RAW264.7 cells stably expressing shRNA targeting the 3′ UTR of *Ifi204* mRNA (*Ifi204* shRNA) resulted in over 95% knockdown of *Ifi204* mRNA (Figure 2B). We transfected these cells with immune-stimulatory DNA derived from vaccinia virus (VV70mer[6]) and measured tumor necrosis factor (TNF) secretion as a readout of the DNA-sensing pathway. DNA-dependent TNF production was significantly impaired in *Ifi204* shRNA cells compared with control cells (Figure 2C), while DNA-independent TNF secretion, stimulated by LPS, was not affected by reduction of IFI204 expression (Figure 2D). These data fit with the previously described role of IFI204 as a dsDNA sensor in RAW264.7 cells.[6] We also generated RAW264.7 cells stably expressing shRNA targeting the 3′ UTR of *Ifi207* mRNA (*Ifi207* shRNA) and obtained about 50% reduction of *Ifi207* mRNA (Figure 2E), which translated into a strong reduction IFI207 protein following LPS stimulation (Figure 2F). Expression of *Ifi207* shRNA in RAW264.7 cells did not significantly affect the expression of other PYHIN genes (Figure S3A). Like *Ifi204*, expression of *Ifi207* shRNA significantly impaired DNA-stimulated TNF secretion (Figure 2G) but also LPS-stimulated TNF secretion (Figure 2H). Analysis of *Tnf* mRNA induction confirmed the requirement of IFI207 for both DNA- and LPS-stimulated responses and indicated a role for IFI207 in transcriptional induction of *Tnf* (Figures 2I and 2J). Importantly, stimulation of cells with further PRR ligands, namely Pam3Cys (for TLR2) or transfected poly(I:C) (for cytosolic RIG-I-like receptors that sense RNA), also showed a dependency on IFI207 for *Tnf* induction (Figures 2K and 2L). This was confirmed by generating RAW264.7 cells expressing a different *Ifi207* shRNA, targeting the coding region of *Ifi207* (*Ifi207* shRNA #2; Figure S3B), which also led to significant impairment of LPS-induced *Tnf* mRNA but did not inhibit LPS-stimulated *Ifnβ* (Figures S3C and S3D). Further, J774 macrophages expressing shRNA targeting *Ifi207* (Figure S3E) also showed that LPS-stimulated *Tnf* mRNA induction and TNF secretion were significantly reduced compared with cells expressing control shRNA (Figures S3F and S3H), while LPS-induced Ccl5 was unaffected (Figures S3G and S3I).

IFI207 regulates *Tnf* promoter induction rather than cytosolic signaling pathways

The shRNA experiments showed a stimulus-independent role for IFI207 in regulation of *Tnf* expression, suggesting that IFI207 would mediate *Tnf* induction by regulating a shared signaling pathway used by multiple PRRs or at a point very proximal to the *Tnf* gene promoter. To test a role for IFI207 in common signaling events known to be required for *Tnf* induction, we stimulated RAW264.7 macrophages with LPS and measured activation of transcription factors nuclear factor κB (NF-κB) and IRF3, and p38 MAP kinase, by western blot. There was no marked reduction in IRF3 activation (as measured by appearance of phosphorylated [phospho]-IRF3) in NF-κB activation (as measured by degradation of IκBα and appearance of phospho-p65) nor in p38 phosphorylation in macrophages expressing *Ifi207* shRNA compared with control shRNA (Figure S4). This suggested that IFI207 more likely acted proximal to *Tnf* promoter induction, consistent with its nuclear expression (Figure 1B). To test this, we examined how knockdown of *Ifi207* in macrophages affects RNA Pol II occupancy of the *Tnf* gene. Thus, we performed chromatin immunoprecipitation (ChIP) of RNA Pol II in control (Ctrl) and *Ifi207* shRNA-expressing J774 cells following LPS stimulation. No reduction of RNA Pol II presence at the *Tnf* promoter nor of RNA Pol II recruitment following LPS stimulation was observed in *Ifi207* shRNA-expressing J774 cells compared with control cells (Figure 2M). However, when the same samples were tested using primers binding within the *Tnf* gene, a significant reduction of actively transcribing RNA Pol II could be seen after 3 h LPS stimulation in IFI207 shRNA cells compared with control cells (Figure 2N), while histone H3 acetylation, a common marker of gene activation, was similar between control and *Ifi207* shRNA cells (Figure 2O).

Overall, the results so far showed that IFI207 regulated *Tnf* gene induction independently of cytosolic signaling pathways but proximal to the gene promoter, being required for optimal RNA Pol II activity on the *Tnf* gene.

Generation of an *Ifi207*$^{-/-}$ mouse reveals a broad role for IFI207 in cytokine transcription

To further explore the role of IFI207 in cytokine gene induction, and to be able to examine the role of IFI207 *in vivo*, we used CRISPR-Cas9 to generate an *Ifi207* knockout mouse, C57BL/6J-Ifi207^{em1Wor} (herein referred to as *Ifi207*$^{-/-}$). Sequence analysis of the *Ifi207*$^{-/-}$ mouse confirmed a disrupted *Ifi207* locus (1,091 nucleotide [nt] deletion spanning exons 2 and 3 of the *Ifi207* gene [Figure 3A]), leading to a frameshift into the coding sequence of *IFI207* and an early STOP codon within exon 4. The *Ifi207*$^{-/-}$ mice were further validated by genotyping using two separate sets of primers (Figure S5A). Importantly, the expression of other PYHIN locus genes apart from *Ifi207* was not significantly affected in the *Ifi207*$^{-/-}$ mice (Figure 3B). Immunoblotting or confocal analysis of iBMDMs generated from *Ifi207*$^{-/-}$ mice confirmed the lack of IFI207 protein expression in both unstimulated and IFNβ- or LPS-stimulated cells (Figures 3C, 3D, and S5B–S5E).

Analysis of cytokine release from *Ifi207*$^{-/-}$ BMDMs in response to LPS or Pam3Cys stimulation revealed a broader role in cytokine secretion for IFI207 beyond just TNF since, as well as TNF secretion, interleukin-6 (IL-6) and IFNβ release were also significantly impaired in knockout (KO) compared with WT cells (Figures 3E–3G, 3I, and 3J). Note that LPS, but not Pam3Cys, elicited IFNβ production from cells. Not all secreted cytokines were IFI207 dependent, as IP10 (CXCL10) release was similar in WT and KO BMDMs (Figures 3H and 3K).

The middle domain of IFI207 protein directly activates cytokine gene promoters

We next examined the direct effect of IFI207 protein expression on cytokine promoter induction by reporter gene analysis in HEK293T cells. This showed that ectopic expression of IFI207

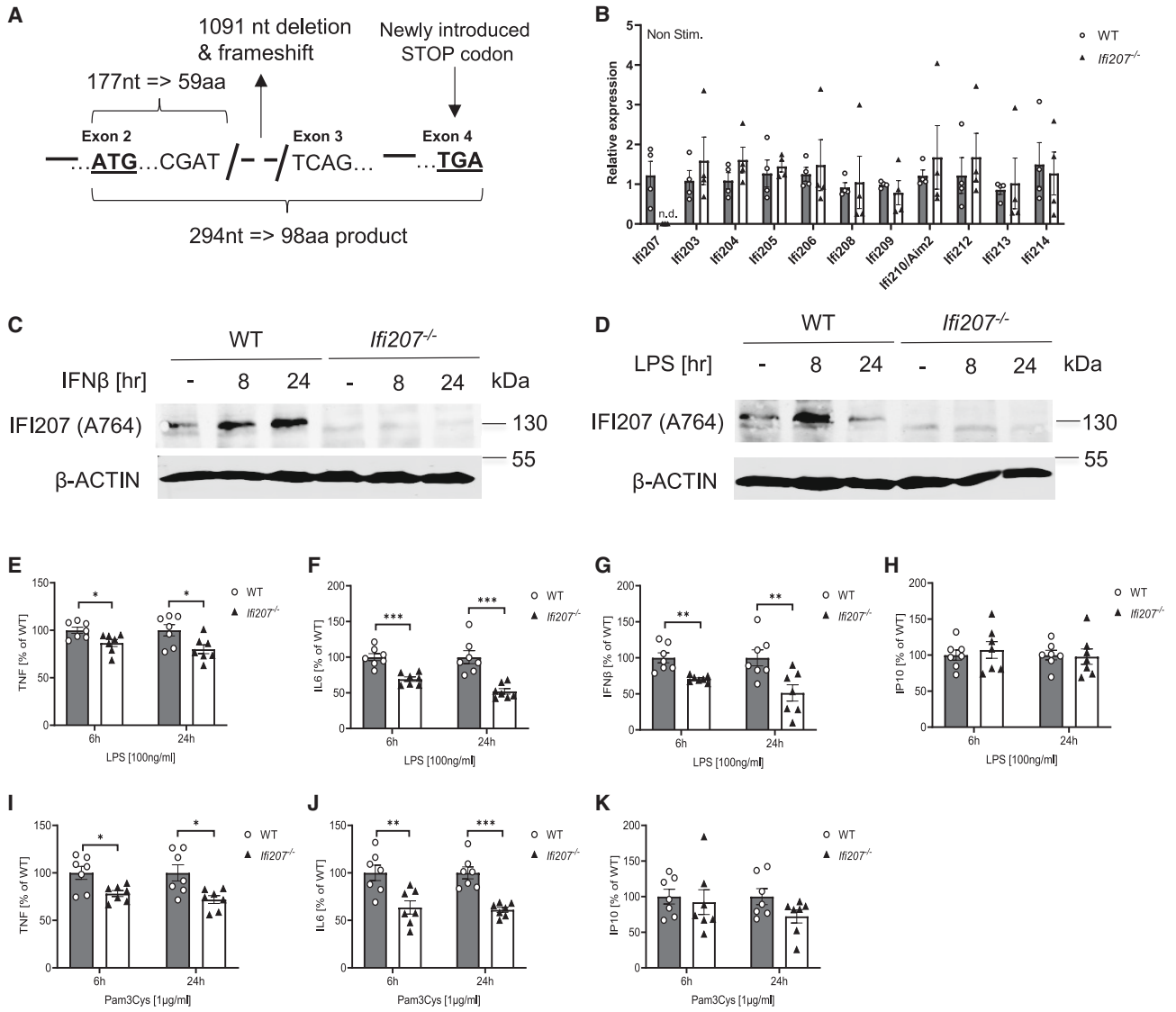

Figure 3. Macrophages from *Ifi207*$^{-/-}$ mice show impaired cytokine responses

(A) Genetic modification in the *Ifi207*$^{-/-}$ mouse. Shown is the location and size of the obtained deletion, spanning exons 2 and 3, resulting in the frameshift of 177 nt into the *Ifi207* sequence and introduction of the new early stop codon within exon 4.

(B) Expression of PYHIN mRNA in WT and *Ifi207*$^{-/-}$ BMDMs. Data shown are the mean ± SEM of 4 mice per group. n.d. indicates that RNA was not detected.

(C and D) Immunoblot analysis of IFI207 in WT and *Ifi207*$^{-/-}$ iBMDMs stimulated with 1000 U/mL IFNβ (C) or 100 ng/mL LPS (D). Representative of 2 independent experiments.

(E–K) WT and *Ifi207*$^{-/-}$ primary BMDMs were stimulated for with 100 ng/mL LPS (E–H) or 1 μg/mL Pam3Cys (I–K), and production of TNF (E and I), IL-6 (F and J), IFNβ (G), and IP10 (H, K) was measured by ELISA. Data shown are mean ± SEM of the percentage of WT cytokine production by BMDMs generated from 7 mice per group across two experiments, with each treatment performed in triplicate. Each dot represents one mouse. Statistical analysis was performed using two-way ANOVA, and *$p < 0.05$, **$p < 0.01$, and ***$p < 0.001$ indicate significance between compared samples.

See also Figure S5.

was sufficient to induce a small, but significant, activation of the *Tnf*, *Ifnβ*, and *IL6* gene promoters (Figures 4A–4H). Further, IFI207 expression significantly enhanced both LPS- and MyD88-stimulated cytokine promoter induction in each case (Figures 4A, 4B, 4E, and 4F). As a negative control, we also examined an *Asc* promoter reporter. The *Asc* gene has previously been shown to be regulated by PYHIN IFI205,[14] and here we found that IFI205, but not IFI207, expression could activate the Asc promoter reporter (Figure 4I).

For PYHINs involved in DNA sensing, the HIN domain is required for direct binding to dsDNA, while the PYD mediates oligomerization after ligand binding,[7,27,28] but what role these domains play in gene promoter regulation is not clear. Thus, we generated truncated versions of IFI207 (Figure 4J) and

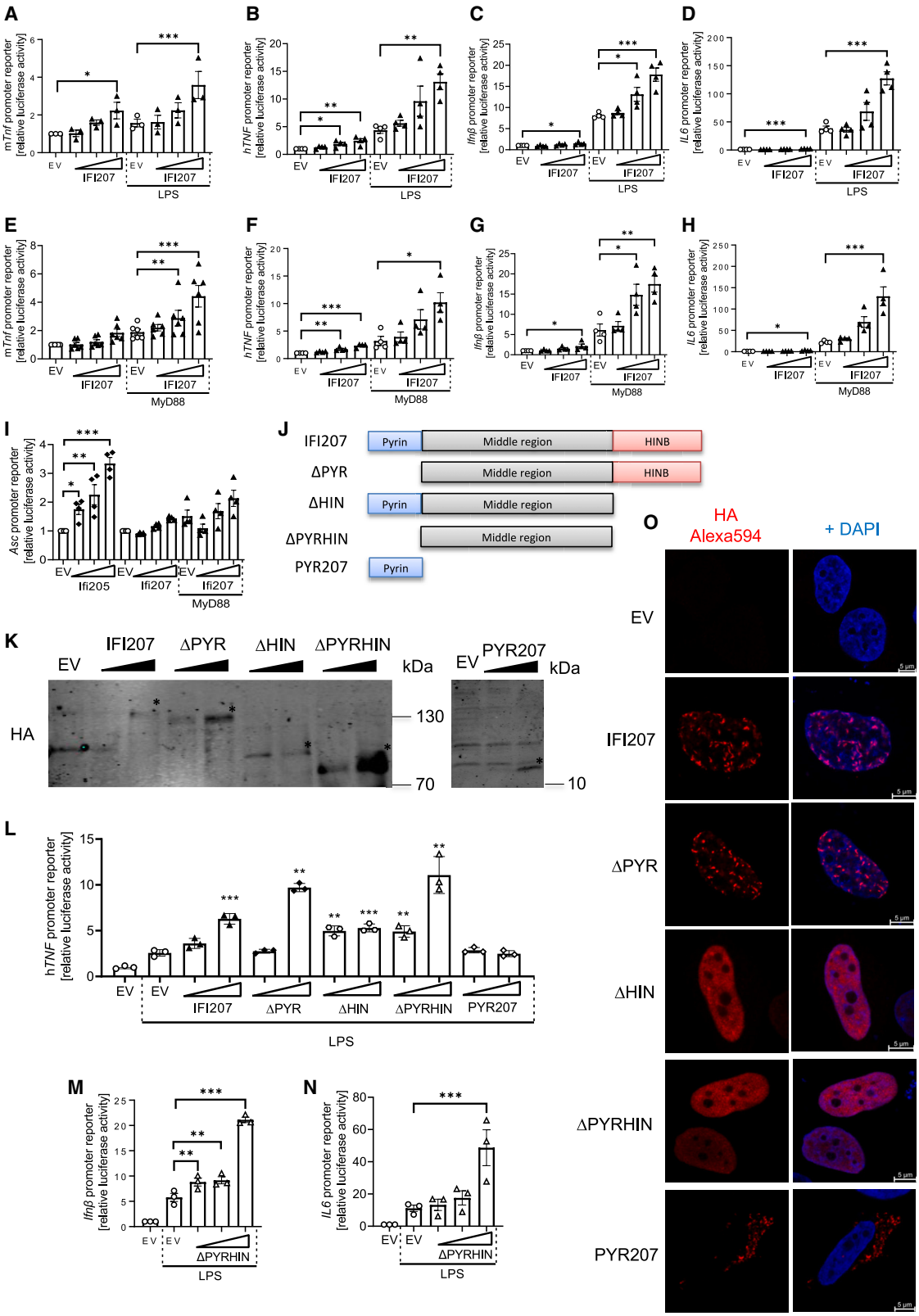

(legend on next page)

confirmed expression of each in transfected cells (Figure 4K). Cells were stimulated with LPS, in order to assess the ability of truncations, compared with full-length IFI207, to enhance LPS-stimulated promoter induction. Surprisingly, truncations lacking either or both the Pyrin or HINB domain could still significantly stimulate activation of the *TNF* promoter (Figure 4L). Of note, ΔPYRHIN, which contains only the middle region of IFI207, was able to boost LPS-stimulated *TNF* promoter activation to a level comparable to the effect of the full-length protein, while the PYD alone (PYR207) did not enhance LPS-induced activation of the *TNF* promoter at all (Figure 4L). Expression of the ΔPYRHIN construct also boosted LPS-stimulated *Ifnβ* and *IL6* gene promoters (Figures 4M and 4N). These data indicate that the middle region alone is sufficient to mediate cytokine promoter induction and that the pyrin and HINB domains are not required.

The HINB and middle domains are required for IFI207 nuclear localization

We also used the set of truncated proteins to determine whether specific domains were required for correct nuclear localization of IFI207, in HeLa cells, by confocal microscopy (Figure 4O). As observed for endogenous IFI207 (Figure 1B), overexpressed full-length IFI207 localized exclusively within the nucleus and showed a speckled pattern of staining (Figure 4O), seen also for the IFI207 lacking the PYD (ΔPYR), but lost when the HINB domain was absent (ΔHIN and ΔPYRHIN). All these constructs still showed nuclear localization, except the PYD alone, suggesting that the middle region of IFI207 represented by ΔPYRHIN is key for its nuclear localization. Further, the HINB domain is required for normal nuclear distribution of IFI207.

IFI207 associates with and co-operates with IRF7 in stimulating promoter activity

Having established that IFI207 regulates transcription of PRR-stimulated cytokine genes from the nucleus, we next explored the mechanism whereby IFI207 might engage with the transcriptional machinery to do this. Induction of many PRR-stimulated cytokine genes involves activation of NF-κB and IRFs, so we examined whether IFI207 could boost the promoter-inducing activity of NF-κB or IRFs. We thus examined the effect of IFI207 on an IFN-stimulated response element (ISRE)-dependent reporter gene, which was shown previously to be transcriptionally activated by IRFs,[29] and on an NF-κB-dependent reporter. Interestingly, when ectopic expression of the kinase TBK1 or IKKε was used to induce the reporters, co-expression of IFI207 had a dramatic and significant enhancing effect on the ISRE reporter compared with a very minor effect on the NF-κB reporter (Figures 5A and 5B). Further, activation of the ISRE reporter by constitutively active IRF7 (IRF7-4D), but not IRF3 (IRF3-5D), was also enhanced by IFI207 expression (Figure 5C). This established a functional relationship between IFI207 and IRF7, and consistent with this, the middle region of IFI207 protein shown to be required for activating cytokine gene promoters (Figures 4L–4N) co-immunoprecipitated with IRF7 (Figure 5D). Furthermore, confocal microscopy showed nuclear co-localization of IFI207 with IRF7 or IRF7-4D (Figures 5E and 5F). Figure 5G confirms that LPS-stimulated TNF secretion is indeed IRF7 dependent in BMDMs. Together, these data suggest that at least one mechanism that accounts for IFI207 regulation of PRR-induced cytokine induction is through association with IRF7, leading to enhanced transcriptional activation.

IFI207 co-localizes with actively transcribing RNA Pol II

Considering the speckled nuclear localization pattern of IFI207, we wondered if this indicated the localization of IFI207 in regions of active gene transcription. During transcription, clusters of active RNA Pol II are marked by hyper-phosphorylation of their C-terminal domains (CTDs), with phosphorylation of S5 and S2 being the most common markers of initiating and elongating enzyme, respectively.[30] We therefore tested whether IFI207 co-localized with either type of active RNA Pol II, in HeLa cells, using confocal microscopy. This showed that IFI207 co-localized with S5-phosphorylated RNA Pol II but not S2-phosphorylated RNA Pol II (Figures 6A and 6B), suggesting an involvement of IFI207 in the early stages of transcriptional initiation at sites of active RNA Pol II in the nucleus, consistent with the role of IRF7 in the initiation of gene transcription.[31]

The absence of IFI207 *in vivo* does not affect the progression of autoimmune disease

Given the cytokine gene regulatory functions of IFI207 in macrophages, we next wanted to assess the physiological role IFI207 *in vivo*. The ability of IFI207 to regulate PRR-stimulated gene

Figure 4. Identification of IFI207 protein domains required for cytokine promoter induction and nuclear localization

(A–I) 293/TLR4-MD2-CD14 (A–D) or HEK293T cells (E–I) were transfected with mouse (A and E) or human (B and F) *Tnf*-promoter, (C and G) *Ifnβ*-promoter, (D and H) *IL6*-promoter, or (I) *Asc*-promoter luciferase reporters and increasing amounts of IFI207-HA (A–I) or Ifi205-hemagglutinin (HA) (I) plasmid (wedge: 50, 100, and 150 ng). Cells were stimulated with 100 ng/mL LPS (A–D) or co-transfected with 25 ng MyD88-expressing vector (E–I), and promoter activation was measured by reporter gene assay. Data shown are the mean ± SEM of 3–6 independent experiments, each performed in triplicate, and statistical analysis was performed using one-way ANOVA.

(J) Schematic of IFI207 truncations generated.

(K) Immunoblot analysis of 293/TLR4-MD2-CD14 cells transfected with 50 or 100 ng (wedge) of plasmids expressing HA-tagged IFI207 truncations for 48 h. Representative of 3 independent experiments.

(L–N) 293/TLR4-MD2-CD14 cells were transfected with human *TNF*-promoter (L), *Ifnβ*-promoter (M), or *IL6*-promoter (N) luciferase reporter and 100 or 150 ng (L) or 50, 100, or 150 ng (M and N) IFI207 truncation plasmids as indicated, followed by stimulation with 100 ng/mL LPS for 24 h. Promoter activation was measured by reporter gene assay. Data shown in (L) are mean ± SD of triplicate samples from a representative of 4 independent experiments, with statistical analysis performed using two-tailed unpaired Student's t test. Data shown in (M) and (N) are mean ± SEM of 3 independent experiments performed in triplicate, with statistical analysis performed using one-way ANOVA. For all panels, *$p < 0.05$, **$p < 0.01$, and ***$p < 0.001$ indicate significance between compared samples.

(O) HeLa cells were transfected with 1 μg IFI207 truncation plasmids, and plasmid expression (red) was detected 24 h post-transfection by confocal microscopy. The nucleus of cells was stained using DAPI (blue). Presented FOV is representative of multiple FOVs taken from 3 independent experiments.

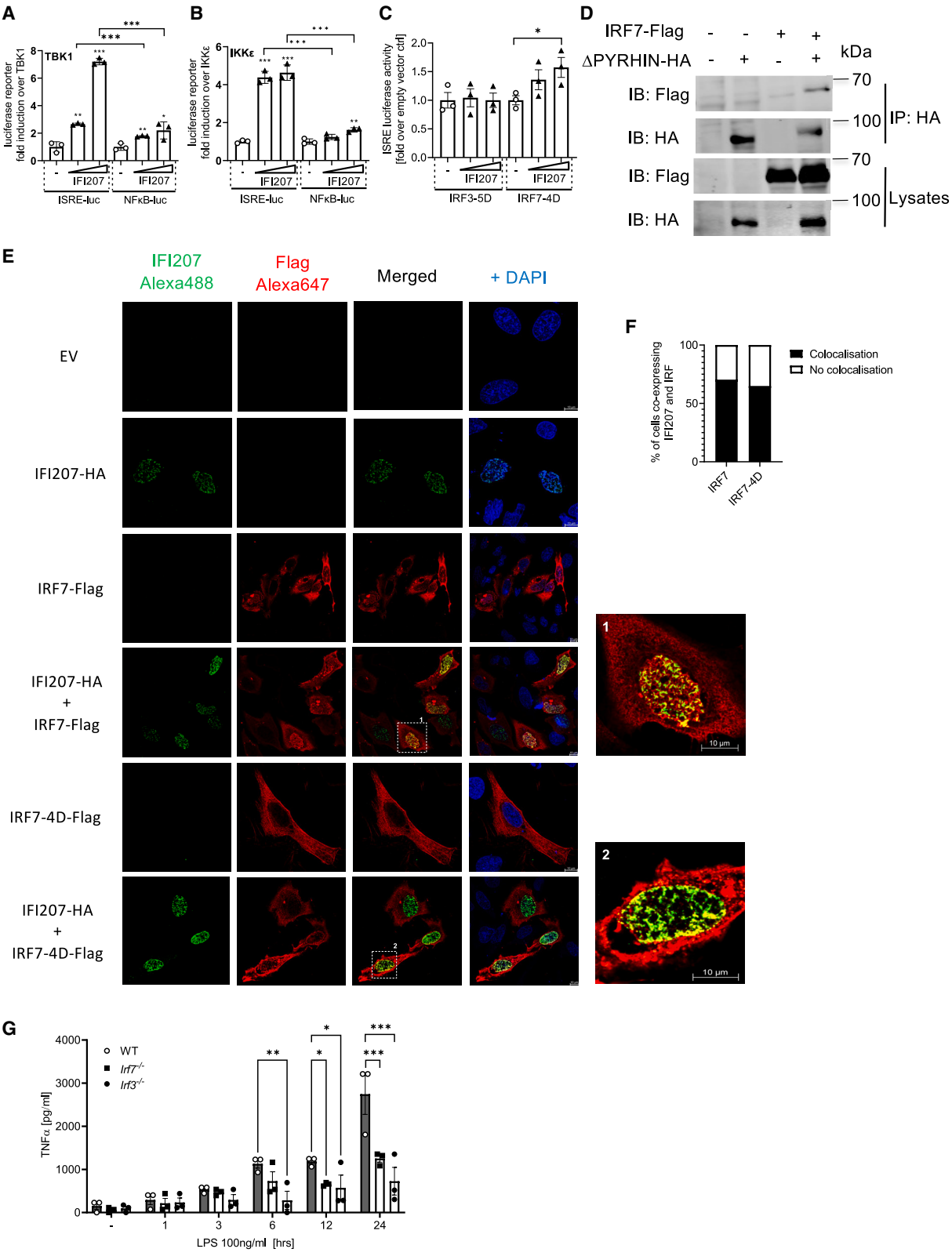

(legend on next page)

induction in macrophages could point to a role for IFI207 in autoimmunity or in pathogen responses *in vivo*. Therefore, we assessed these two possibilities using mouse models of both autoimmunity and infection. For the former, we chose EAE, especially relevant since AIM2 deficiency resulted in exacerbation of CNS inflammation and pathogenesis of EAE[23] and since induction of pro-inflammatory cytokines in the CNS is one of the hallmarks of EAE pathogenesis. WT and *Ifi207*$^{-/-}$ mice were immunized with $MOG_{35–55}$ and pertussis toxin (PT), and mice were scored for EAE and weighed regularly for 17 days (Figure S6A). Both WT and *Ifi207*$^{-/-}$ immunized animals showed a progressive development of EAE and corresponding gradual weight loss compared with naive control mice (Figures S6B and S6C). However, we did not observe any significant difference in EAE pathogenesis between WT and *Ifi207*$^{-/-}$ mice. We also measured pro-inflammatory gene expression in brains isolated from WT and *Ifi207*$^{-/-}$ mice at day 17 of EAE and detected no difference by qRT-PCR (Figures S6D–S6O).

These data show that IFI207 is not involved in development of EAE and regulation of immune gene expression in the brain in the context of autoimmune disease.

IFI207 promotes *K. pneumoniae* infection *in vivo*

To assess a role for IFI207 in pathogen responses *in vivo*, we considered *K. pneumoniae* infection since we observed *in vitro* that *K. pneumoniae* infection significantly induced IFI207 expression in both primary BMDMs and BMDCs (Figures 1G, 1K, and 1M). We used strain Kp52145, which causes invasive infections.[32,33] We first examined the role of IFI207 in gene induction responses to *K. pneumoniae* infection of macrophages by infecting WT and *Ifi207*$^{-/-}$ primary BMDMs and measuring immune gene induction. *Klebsiella*-stimulated *Tnf* and *Ifnb* induction was significantly impaired in cells lacking IFI207 (Figures 7A and 7D). The degree of inhibition of gene induction in cells lacking IFI207 was much more marked for *Klebsiella* compared with LPS, and induction of other immune genes were also potently inhibited (*Il1b*, *Cxcl10*, *Ifit1*, and *Il10*; Figures 7B, 7C, 7E, and 7F).

We next tested how lack of IFI207 would affect *K. pneumoniae* infection *in vivo*. Mice were infected intranasally, and bacterial burden as well as immune gene expression in the lungs of infected mice were examined (Figure 7G). Interestingly, *Ifi207*$^{-/-}$ mice had significantly less bacteria in the lungs 24 h post-infection, suggesting a more efficient clearance of the bacteria in the absence of IFI207 and a need of IFI207 for *Klebsiella* to establish infection (Figure 7H). Additionally, there was reduced expression of *Tnf*, *Il1*, *Ifnb*, *Il10*, and *Ifit1* in the lungs of *Ifi207*$^{-/-}$ mice compared with WT mice (Figures 7I–7M), consistent with the previous results in primary BMDMs. Not all genes were reduced, as expression of *Il12* mRNA was increased (Figure 7N). It has recently been shown that *Klebsiella* needs to infect lung macrophages in order to establish an infection *in vivo*.[34] Since the data thus far showed that IFI207 was needed to establish lung infection and that the absence of IFI207 suppressed *Klebsiella*-stimulated gene induction far more than was the case for LPS stimulation of cells, we wondered whether IFI207, as well as regulating macrophage cytokine induction, might also additionally have a role in bacterial entry or survival in macrophages. Interestingly, although adhesion of bacteria to macrophages was unaffected by the absence of IFI207 (Figure 7O), as was cellular survival (Figure 7Q), phagocytosis of *Klebsiella* was significantly impaired in *Ifi207*$^{-/-}$ macrophages compared with WT cells (Figure 7P), while bacterial-induced phosphorylation of AKT, a marker of phagocytosis of *Klebsiella*,[35] was also impaired (Figure 7R).

We also examined a potential role for IFI207 in *S. aureus* infection *in vitro* and *in vivo*. Only a subtle effect of IFI207 on *S. aureus*-stimulated cytokine induction was seen *in vitro*, whereby there was no significant difference in cytokine induction in infected macrophages, except for *Ifnb* (Figures S7A–S7F). Further, there was no difference in bacterial load in lungs of *S. aureus*-infected *Ifi207*$^{-/-}$ and WT mice (Figure S7G), nor was there any difference in cytokine induction in infected lungs (Figures S7H–S7M). Consistent with this lack of effects *in vivo*, unlike *Klebsiella*, there was no role for IFI207 in macrophage phagocytosis of *S. aureus* (Figure S7O), while bacterial adhesion and intracellular survival were also normal in *Ifi207*$^{-/-}$ macrophages (Figures S7I and S7P).

Together, the results implicate IFI207 as a PYHIN protein involved in regulation of innate immune responses, define protein domains required for PYHIN regulation of cytokine gene induction, show that IFI207 cooperates with IRF7 to enhance transcription, and demonstrate a role for IFI207 in the establishment of a bacterial lung infection *in vivo*.

DISCUSSION

Apart from AIM2, the role of the majority of mouse PYHIN proteins is still poorly understood, while it is unclear how different

Figure 5. IFI207 associates with and co-operates with IRF7 in stimulating promoter activity

(A–C) HEK293T cells were transfected with ISRE- or NF-κB-dependent reporter genes and IFI207-HA plasmid (25 or 50 ng). Cells were stimulated by co-transfecting them with 10 ng TBK1 (A) or IKKε (B) or with 25 ng IRF3-5D or IRF7-4D (C) expression vectors for 24 h. Promoter activation was measured by reporter gene assay. Data shown are mean ± SEM of 3 independent experiments performed in triplicate. Statistical analysis was performed using two-tailed unpaired Student's t test.

(D) Co-immunoprecipitation of IRF7 with the middle region of IFI207 (ΔPyrHIN). HEK293T cells were transfected with 4 μg ΔPyrHIN-HA and/or IRF7-FLAG expression plasmids and lysates immunoprecipitated with αHA antibody 48 h later. Representative of 4 independent experiments.

(E and F) Confocal microscopy of HeLa cells transfected with 0.5 μg IFI207-HA (green) and 0.5 μg IRF7-FLAG or IR7-4D-FLAG (red) expression plasmids (E) showing co-localization of IFI207-HA with IRF7-FLAG or IRF7-4D-FLAG (yellow). Dashed boxes labeled 1 and 2 mark zoomed-in areas shown on the side of the figure. (F) Percentage of cells expressing both IFI207-HA and IRF7-FLAG or IRF7-4D-FLAG and showing co-localization (black) or no co-localization (white) was calculated based on multiple FOVs from 4 independent experiments.

(G) TNF secretion (ELISA) in LPS-stimulated WT, *Irf7*$^{-/-}$, and *Irf3*$^{-/-}$ iBMDMs. Data shown are mean ± SEM of 3 independent experiments performed in triplicate. Statistical analysis was performed using two-way ANOVA.

For all panels, *p < 0.05, **p < 0.01, and ***p < 0.001 indicate significance between compared samples.

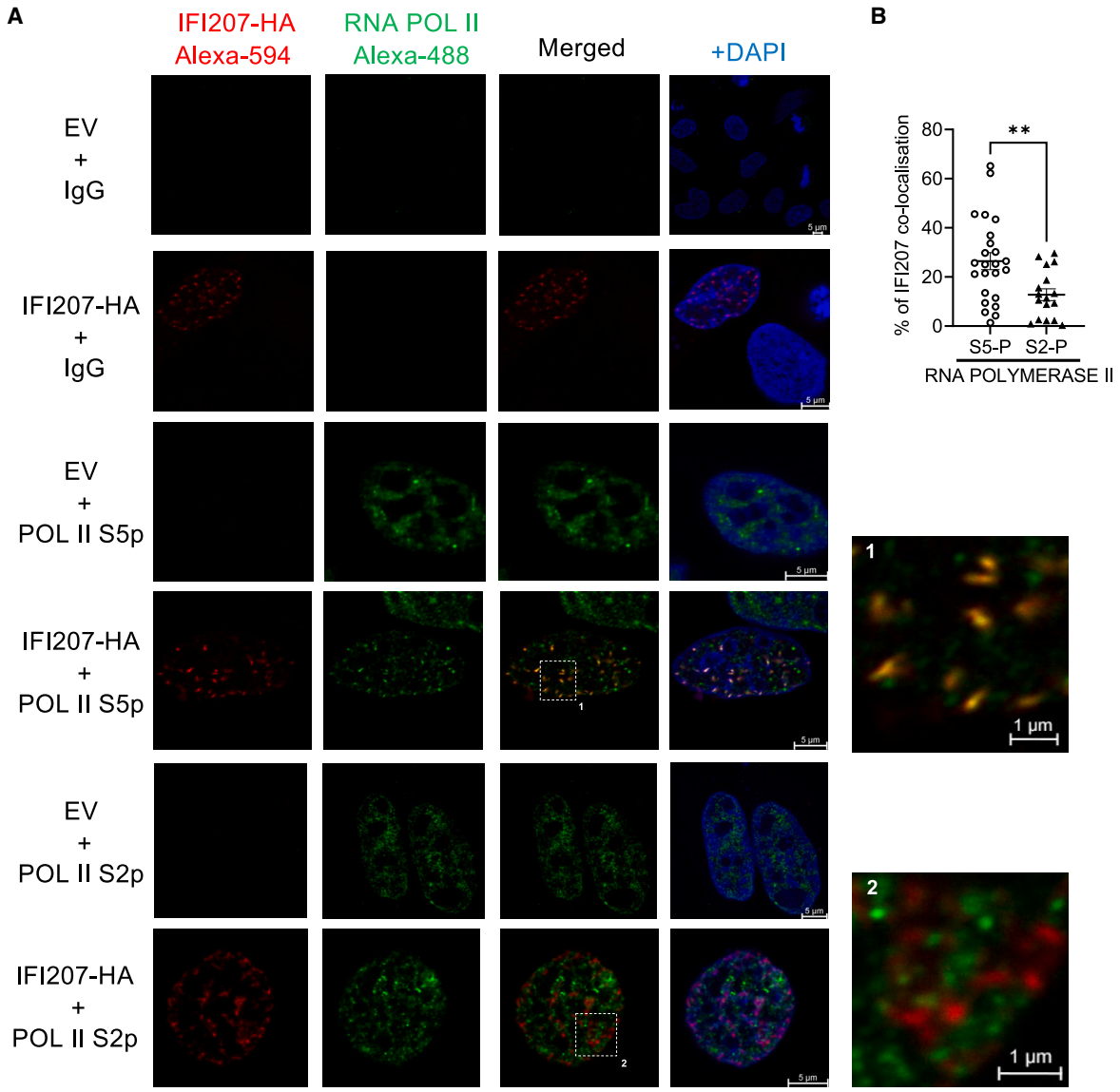

Figure 6. IFI207 co-localizes with actively transcribing RNA Pol II

(A) Confocal microscopy of HeLa cells transfected with 1 μg IFI207-HA plasmid and stained for IFI207 expression (red) and endogenous RNA Pol II S5p or S2p (green). Yellow represents co-localization of IFI207-HA with RNA Pol II. Dashed boxes labeled 1 and 2 mark zoomed-in areas shown on the side of the figure. (B) Percentage of IFI207 co-localization with RNA Pol II S5p (n = 24 FOVs) or S2p (n = 17 FOVs) from 4 independent experiments was quantified using ImageJ and presented as mean ± SEM. Statistical analysis was performed using two-tailed unpaired Student's t test, and **$p < 0.01$ indicates significance between compared samples.

PYHINs, which share similar protein domain structures, can have very different functions ranging from innate immune DNA sensing to viral restriction to regulation of host genes. Our study makes the following specific contributions to our understanding of how PYHINs regulate immune responses: (1) we characterize the function of IFI207 as a transcriptional regulator of cytokine genes; (2) we identify the protein domains that contribute to the ability of IFI207 to regulate transcription; (3) we show that IFI207 associates with IRF7 and actively transcribes RNA Pol II and is required for transcriptional initiation from the promoter rather than RNA Pol II recruitment to the promoter; and (4) we reveal an *in vivo* role for IFI207 in the establishment of a *Klebsiella* infection.

We initially focused on IFI207 since it was more highly expressed in macrophages than other cell types examined and was inducible by PAMPs and pathogens. Other mouse PYHINs expressed preferentially in myeloid cells are IFI204 and IFI205, which have previously been shown to sense dsDNA and regulate *Asc* gene transcription respectively.[6,14] Loss-of-function and gain-of-function experiments indicated that IFI207 was required to induce the Tnf, and other cytokine, gene promoters in response to activation of PRR signaling pathways. This

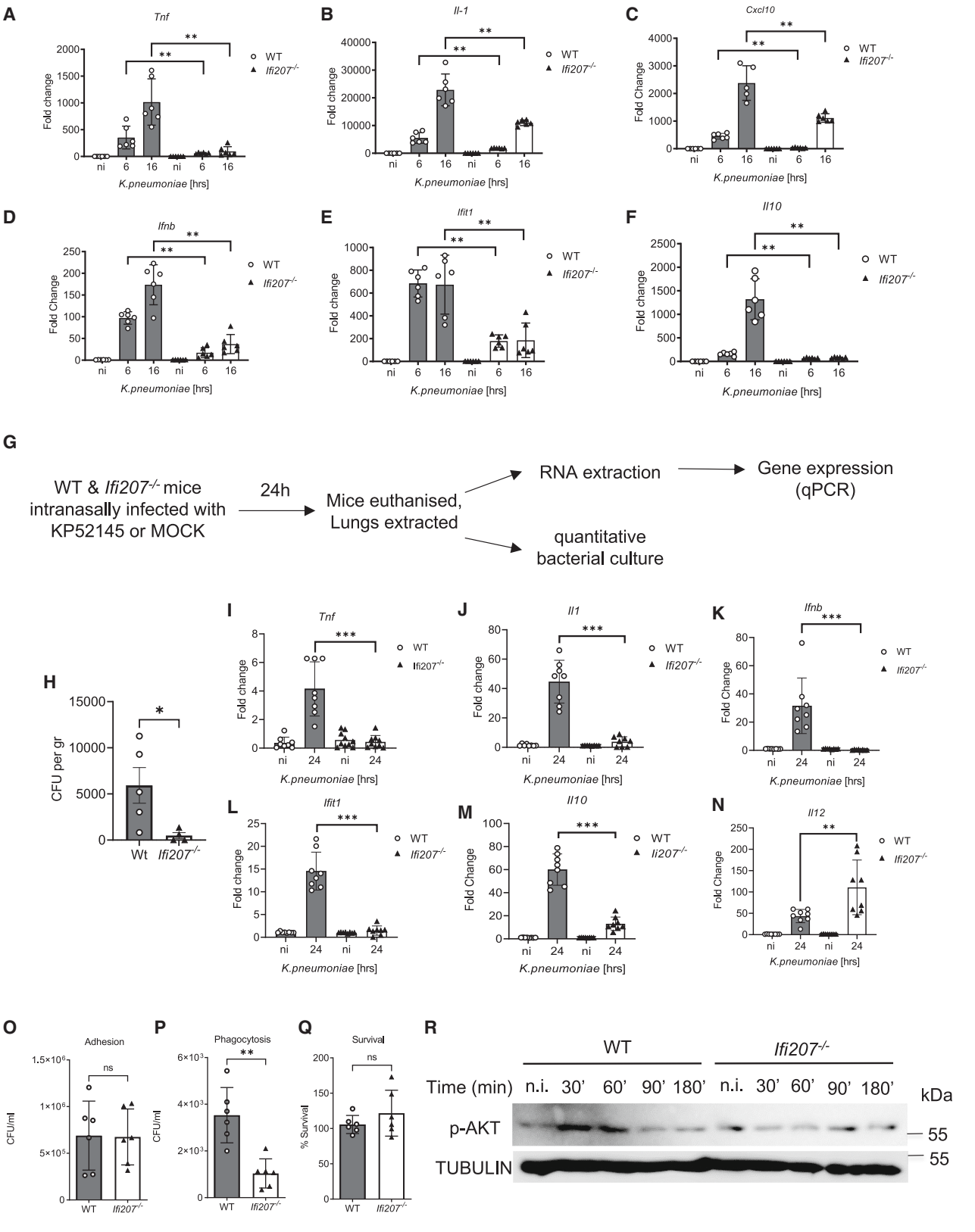

(legend on next page)

contrasted with IFI204, which was only required for DNA-stimulated Tnf induction.

IFI207 is thus added to a growing list of human (IFI16, MNDA, PYHIN1) and mouse (IFI205, IFI204, IFI202) PYHINs shown to modulate gene induction.[12,14,16,17,36–38] IFI207 was visible in characteristic puncta in the nucleus and co-localized with transcriptionally active S5p RNA Pol II, pointing to a transcriptional role for IFI207 in the regulation of gene expression. Interestingly, IFI207 did not co-localize with S2p RNA Pol II, which is a post-translational modification of RNA Pol II characteristic of an actively elongating enzyme.[39] This could mean that IFI207 affects gene expression at the level of transcriptional initiation, which is consistent with the ChIP data that showed a reduced amount of LPS-stimulated RNA Pol II along the *Tnf* gene, even though the presence of RNA Pol II at the *Tnf* promoter was similar in IFI207-sufficient and -deficient cells. Therefore, IFI207 could be required to boost transition of RNA Pol II out of the promoter and into the coding region of the gene in response to PRR stimulation.

A key unresolved issue is how do different PYHINs with largely similar conserved protein domains (the PYD and HIN domains) specifically regulate different genes? In some cases, PYHINS have been shown to associate with transcription factors; for example, IFI16 sequesters Sp1 to restrict HIV-1 and to regulate induction of the IκBα gene.[12,15] This requires both the PYD of IFI16 and the linker region between the PYD and HIN domain.[40] Further, human MNDA was found to interact with the Ying Yang 1 (YY1) transcription factor in a PYD- and HIN-independent manner, leading to increased binding of YY1 to gene promoters.[41] Thus, regions outside of the PYD and HIN domains may define the gene-specific transcriptional roles of PYHINs due to such regions facilitating interactions with the transcriptional machinery and consistent with us finding that the middle region of IFI207 between the PYD and the HIN domain was necessary to induce the *Tnf* promoter. Interestingly, IFI207 associated with IRF7 via this middle region, co-localized with IRF7 in the nucleus, and boosted IRF7-dependent promoter activity. The ability of IFI207 to cooperate with IRF7 likely accounts for at least some of the effects of IFI207 on cytokine transcription, and we confirmed that LPS-stimulated Tnf induction was indeed IRF7 dependent. Previously, we showed that human PYHIN MNDA also regulated IRF7, but in that case, MNDA was actually required for transcription of the *IRF7* gene.[16] Thus, PYHINs regulate IRF7-dependent innate immune pathways but via different mechanisms in mouse and human.

Generation of an *Ifi207*$^{-/-}$ mouse allowed us to evaluate the effects of lack of IFI207 on development of autoimmune disease and on pathogen infection and showed that the role of IFI207 *in vivo* is distinct from both AIM2 and IFI204. Recently, mouse AIM2 has been described to negatively regulate pathogenesis of EAE by inflammasome-independent regulation of Treg cell fate and microglia activation.[23,24] EAE is a T cell-driven disease; however, the pro-inflammatory cytokines produced by myeloid cells within the CNS can also have a significant impact on its development.[42] *Ifi207*$^{-/-}$ mice showed no difference in EAE scores, weight loss, and immune gene induction in brains of affected mice compared with WT control, suggesting no role for IFI207 in T cell regulation as it relates to EAE or for cytokine induction in the brain.

In terms of pathogen infection, previously, IFI204 was shown to contribute to the control of pulmonary bacterial infection, as *Ifi204*$^{-/-}$ mice infected with *S. aureus* showed reduced cytokine responses and increased bacterial burdens in lungs compared with WT mice.[43] However, in contrast to the protective role of IFI204 for *S. aureus*, here we found no role for IFI207 for *S. aureus*, while pulmonary infection with *K. pneumoniae* resulted in a significant reduction of bacterial loads in lungs of *Ifi207*$^{-/-}$ mice compared with WT mice. The results show that IFI207 plays a strong negative role in the regulation of bacterial clearance in the lung and suggests that *K. pneumoniae* could utilize IFI207 to establish a successful infection. The *in vivo* data presented here demonstrate that different PYHINs can have very distinct roles despite their structural and sequence similarities and highlight the need to better characterize the whole mouse locus, one gene at a time.

For *Klebsiella,* cytokine responses both in isolated cells and *in vivo* in lungs were strongly impaired in *Ifi207*$^{-/-}$ mice compared with WT mice, in fact much more so than in the case of cytokine responses to LPS in *Ifi207*$^{-/-}$ BMDMs. There were at least two possible explanations for the discrepancy

Figure 7. IFI207 promotes *K. pneumoniae* infection *in vivo*

(A–F) BMDMs from WT and *Ifi207*$^{-/-}$ mice were infected with 100 MOI of *K. pneumoniae* and mRNA expression of *Tnf* (A), *Il1* (B), *Cxcl10* (C), *Ifnb* (D), *Ifit1* (E), and *Il10* (F) was measured by qPCR. Data present the mean ± SD of cells isolated from 3 mice each performed in duplicate. Statistical analysis was performed using Mann-Whitney test.

(G) *K. pneumoniae* pulmonary infection model.

(H) Quantitative bacterial culture analysis of lung tissue from *K. pneumoniae*-infected WT and *Ifi207*$^{-/-}$ mice. Data show bacterial burden as CFU per gram of tissue from 4–5 mice and are mean ± SEM. Statistical analysis was performed using two-tailed unpaired Student's t test.

(I–N) mRNA expression of *Tnf* (I), *Il1* (J), *Ifnb* (K), *Ifit1* (L), *Il10* (M), and *Il12* (N) measured in lung tissue from *K. pneumoniae*-infected and uninfected WT and *Ifi207*$^{-/-}$ mice by qPCR. Data are presented as mean ± SD of 8–9 mice. Statistical analysis was performed using one-way ANOVA.

(O–Q) WT and *Ifi207*$^{-/-}$ iBMDMs were infected with *K. pneumoniae* for 30 min, washed, and lysed immediately (O) or following 30 min (P) or 5 h (Q) incubation in the medium containing gentamicin (100 μg/mL) to kill extracellular bacteria. Data in (O) and (P) are shown as mean ± SD of CFU/mL from 3 independent experiments performed in duplicate. Data in (Q) show mean ± SD of the percentage of survival from 3 independent experiments performed in duplicate and calculated as CFUs in *Ifi207*$^{-/-}$ cells at 5 h versus 30 min and normalized to the results obtained for WT macrophages set to 100%. Statistical analysis was performed using two-tailed unpaired Student's t test. For all graphs, *$p < 0.05$, **$p < 0.01$, and ***$p < 0.001$ indicate significance between compared samples. n.s. indicates no significant difference.

(R) Immunoblot of AKT phosphorylation and tubulin expression in WT and *Ifi207*$^{-/-}$ macrophages following infection with *K. pneumoniae*. Representative of 3 independent experiments.

See also Figure S7.

between LPS and *Klebsiella*. Since *K. pneumoniae* is a more complex stimuli than LPS that would activate multiple PRR pathways, and since the mammalian innate immune system evolved under pressure from such pathogens rather than from purified PRR ligands, the data could reveal a more potent role for IFI207 in cytokine induction than seen for pure PMAPs. Alternatively, the discrepancy could be due to a reduced uptake of *Klebsiella* by *Ifi207*$^{-/-}$ macrophages compared with WT macrophages, thus having a knock-on effect on bacterial-induced host genes. Evidence for the latter explanation was obtained since, although adhesion and intracellular survival of *Klebsiella* were similar for WT and KO cells, phagocytosis was severely impaired in the KO cells. Why exactly IFI207 is required for *Klebsiella* phagocytosis is unclear, especially since *S. aureus* phagocytosis was normal in *Ifi207*$^{-/-}$ macrophages, but one likely explanation is that IFI207 transcriptionally regulates host genes specifically required for *Klebsiella* phagocytosis. Proving initial support, here we have shown that the phosphorylation of AKT, essential for the phagocytosis of *Klebsiella*,[35] is impaired in *Ifi207*$^{-/-}$ macrophages. Impaired macrophage phagocytosis of *Klebsiella* in the absence of IFI207 *in vitro* provided a potential explanation for the dramatic effect of the absence of IFI207 *in vivo* on the progression of *Klebsiella* infection since it has recently been shown that *Klebsiella* needs to infect lung macrophages in order to establish pulmonary infection.[34]

In conclusion, we have shown that IFI207 functions as a transcriptional regulator of immune gene expression, proximal to transcriptionally active RNA Pol II, and engages with IRF7. Additionally, IFI207 has a significant impact on the establishment of a pulmonary bacterial infection *in vivo*. Overall, the study emphasizes the emerging role of PYHINs as critical regulators of cytokine response to pathogens and adds mechanistic insights into how PYHINs regulate innate immunity.

Limitations of the study

We showed that IFI207 regulates induction of cytokine promoters and that IFI207 co-localizes with active RNA Pol II in the nucleus. However, the level of endogenous IFI207 protein expression, together with the sub-optimal efficacy of the IFI207 antibodies, precluded us from being able to assess whether endogenous IFI207 directly associates with cytokine promoters or acts more distally, for example through regulation of IRF7 activity in the nucleus. We excluded a role for IFI207 in autoimmunity *in vivo* using an EAE model. In order to definitively exclude a role for IFI207 in autoimmunity, other mouse models should also be tested. We hypothesize that the role of IFI207 in establishing a *Klebsiella* infection *in vivo* is related to not only reduced cytokine induction but also an inability of *Ifi207*$^{-/-}$ BMDMs to phagocytose *Klebsiella in vitro*. This activity likely makes a strong contribution to the requirement *Klebsiella* has for IFI207 *in vivo*, but this remains to be proven. Further, the mechanism whereby IFI207 is required for *K. pneumoniae*, but not *S. aureus*, phagocytosis is unclear.

STAR★METHODS

Detailed methods are provided in the online version of this paper and include the following:

- KEY RESOURCES TABLE
- RESOURCE AVAILABILITY
  - Lead contact
  - Materials availability
- EXPERIMENTAL MODEL AND SUBJECT DETAILS
  - Animal model
  - Primary cells
  - Cell lines
  - Bacterial strains
- METHOD DETAILS
  - Cell treatments with stimulants and bacteria
  - Bacterial adhesion, phagocytosis and survival
  - Generation of PYHIN shRNA-expressing cells
  - Cloning of IFI207 and its truncations
  - Generation of IFI207 antibody
  - ELISA for cytokine secretion
  - RNA analysis by quantitative RT-PCR
  - Immunoblotting
  - Co-immunoprecipitation
  - Chromatin immunoprecipitation
  - Reporter gene assay
  - Confocal microscopy
  - Flow cytometry
  - Generation and use of *Ifi207*$^{-/-}$ mice
  - Experimental autoimmune encephalomyelitis (EAE)
  - Intranasal infection of mice with bacteria
  - Bioinformatics
- QUANTIFICATION AND STATISTICAL ANALYSIS
  - Data availability

SUPPLEMENTAL INFORMATION

Supplemental information can be found online at https://doi.org/10.1016/j.celrep.2023.112341.

ACKNOWLEDGMENTS

Confocal imaging was performed at the TBSI Microscopy and Imaging Centre, with technical assistance from Gavin McManus. Flow cytometry was performed in the TBSI Flow Cytometry Facility, with technical assistance from Barry Moran and Aoife O'Rourke. We thank members of the Bowie lab for helpful discussions. This work was funded by Science Foundation Ireland (SFI; 11/PI/1056, 15/SPP/3212, and 16/IA/4376 to A.G.B., 15/IA/3041 to R.M.M., and 16/IA/4468 to K.H.G.M.); The Wellcome Trust (202846/Z/16/Z to R.M.M.); the Medical Research Council (MR/V032496/1 to J.A.B.); the Biotechnology and Biological Sciences Research Council (BBSRC; BB/T001976/1 to J.A.B.); and a BBSRC-SFI joint award (17/BBSRC/3414 to A.G.B. and BB/P020194/1 to J.A.B.).

AUTHOR CONTRIBUTIONS

Conceptualization, M.B., A.G.B., and J.A.B.; methodology, M.B. and Z.J.; investigation, M.B., C.F., A.McG., R.C.-G., A.D., C.E.S., S.R.C., J.S.P., and J.K.; writing – original draft, M.B., A.G.B., and J.A.B.; writing – review and editing, M.B., A.G.B., R.M.M., and J.A.B.; supervision, K.H.G.M., K.A.F., R.M.M., J.A.B., and A.G.B.; funding acquisition, A.G.B.

DECLARATION OF INTERESTS

The authors declare no competing interests.

Received: March 24, 2022
Revised: February 2, 2023
Accepted: March 20, 2023

REFERENCES

1. Keating, S.E., Baran, M., and Bowie, A.G. (2011). Cytosolic DNA sensors regulating type I interferon induction. Trends Immunol. *32*, 574–581. https://doi.org/10.1016/j.it.2011.08.004.
2. Cridland, J.A., Curley, E.Z., Wykes, M.N., Schroder, K., Sweet, M.J., Roberts, T.L., Ragan, M.A., Kassahn, K.S., and Stacey, K.J. (2012). The mammalian PYHIN gene family: phylogeny, evolution and expression. BMC Evol. Biol. *12*, 140. https://doi.org/10.1186/1471-2148-12-140.
3. Brunette, R.L., Young, J.M., Whitley, D.G., Brodsky, I.E., Malik, H.S., and Stetson, D.B. (2012). Extensive evolutionary and functional diversity among mammalian AIM2-like receptors. J. Exp. Med. *209*, 1969–1983. https://doi.org/10.1084/jem.20121960.
4. Choubey, D., Duan, X., Dickerson, E., Ponomareva, L., Panchanathan, R., Shen, H., and Srivastava, R. (2010). Interferon-inducible p200-family proteins as novel sensors of cytoplasmic DNA: role in inflammation and autoimmunity. J. Interferon. Cytokine Res. *30*, 371–380. https://doi.org/10.1089/jir.2009.0096.
5. Ludlow, L.E.A., Johnstone, R.W., and Clarke, C.J.P. (2005). The HIN-200 family: more than interferon-inducible genes? Exp. Cell Res. *308*, 1–17. https://doi.org/10.1016/j.yexcr.2005.03.032.
6. Unterholzner, L., Keating, S.E., Baran, M., Horan, K.A., Jensen, S.B., Sharma, S., Sirois, C.M., Jin, T., Latz, E., Xiao, T.S., et al. (2010). IFI16 is an innate immune sensor for intracellular DNA. Nat. Immunol. *11*, 997–1004. https://doi.org/10.1038/ni.1932.
7. Hornung, V., Ablasser, A., Charrel-Dennis, M., Bauernfeind, F., Horvath, G., Caffrey, D.R., Latz, E., and Fitzgerald, K.A. (2009). AIM2 recognizes cytosolic dsDNA and forms a caspase-1-activating inflammasome with ASC. Nature *458*, 514–518. https://doi.org/10.1038/nature07725.
8. Kerur, N., Veettil, M.V., Sharma-Walia, N., Bottero, V., Sadagopan, S., Otageri, P., and Chandran, B. (2011). IFI16 acts as a nuclear pathogen sensor to induce the inflammasome in response to Kaposi Sarcoma-associated herpesvirus infection. Cell Host Microbe *9*, 363–375. https://doi.org/10.1016/j.chom.2011.04.008.
9. Gariano, G.R., Dell'Oste, V., Bronzini, M., Gatti, D., Luganini, A., De Andrea, M., Gribaudo, G., Gariglio, M., and Landolfo, S. (2012). The intracellular DNA sensor IFI16 gene acts as restriction factor for human cytomegalovirus replication. PLoS Pathog. *8*, e1002498. https://doi.org/10.1371/journal.ppat.1002498.
10. Lo Cigno, I., De Andrea, M., Borgogna, C., Albertini, S., Landini, M.M., Peretti, A., Johnson, K.E., Chandran, B., Landolfo, S., and Gariglio, M. (2015). The nuclear DNA sensor IFI16 acts as a restriction factor for human papillomavirus replication through epigenetic modifications of the viral promoters. J. Virol. *89*, 7506–7520. https://doi.org/10.1128/JVI.00013-15.
11. Johnson, K.E., Bottero, V., Flaherty, S., Dutta, S., Singh, V.V., and Chandran, B. (2014). IFI16 restricts HSV-1 replication by accumulating on the hsv-1 genome, repressing HSV-1 gene expression, and directly or indirectly modulating histone modifications. PLoS Pathog. *10*, e1004503. https://doi.org/10.1371/journal.ppat.1004503.
12. Hotter, D., Bosso, M., Jønsson, K.L., Krapp, C., Stürzel, C.M., Das, A., Littwitz-Salomon, E., Berkhout, B., Russ, A., Wittmann, S., et al. (2019). IFI16 targets the transcription factor Sp1 to suppress HIV-1 transcription and latency reactivation. Cell Host Microbe *25*, 858–872.e13. https://doi.org/10.1016/j.chom.2019.05.002.
13. Ludlow, L.E., Hii, L.L., Thorpe, J., Newbold, A., Tainton, K.M., Trapani, J.A., Clarke, C.J.P., and Johnstone, R.W. (2008). Cloning and characterisation of Ifi206: a new murine HIN-200 family member. J. Cell. Biochem. *103*, 1270–1282. https://doi.org/10.1002/jcb.21512.
14. Ghosh, S., Wallerath, C., Covarrubias, S., Hornung, V., Carpenter, S., and Fitzgerald, K.A. (2017). The PYHIN protein p205 regulates the inflammasome by controlling Asc expression. J. Immunol. *199*, 3249–3260. https://doi.org/10.4049/jimmunol.1700823.
15. Caposio, P., Gugliesi, F., Zannetti, C., Sponza, S., Mondini, M., Medico, E., Hiscott, J., Young, H.A., Gribaudo, G., Gariglio, M., and Landolfo, S. (2007). A novel role of the interferon-inducible protein IFI16 as inducer of proinflammatory molecules in endothelial cells. J. Biol. Chem. *282*, 33515–33529. https://doi.org/10.1074/jbc.M701846200.
16. Gu, L., Casserly, D., Brady, G., Carpenter, S., Bracken, A.P., Fitzgerald, K.A., Unterholzner, L., and Bowie, A.G. (2022). Myeloid cell nuclear differentiation antigen controls the pathogen-stimulated type I interferon cascade in human monocytes by transcriptional regulation of IRF7. Nat. Commun. *13*, 14. https://doi.org/10.1038/s41467-021-27701-x.
17. Massa, D., Baran, M., Bengoechea, J.A., and Bowie, A.G. (2020). PYHIN1 regulates pro-inflammatory cytokine induction rather than innate immune DNA sensing in airway epithelial cells. J. Biol. Chem. *295*, 4438–4450. https://doi.org/10.1074/jbc.RA119.011400.
18. Zhang, W., Cai, Y., Xu, W., Yin, Z., Gao, X., and Xiong, S. (2013). AIM2 facilitates the apoptotic DNA-induced systemic lupus erythematosus via arbitrating macrophage functional maturation. J. Clin. Immunol. *33*, 925–937. https://doi.org/10.1007/s10875-013-9881-6.
19. Kimkong, I., Avihingsanon, Y., and Hirankarn, N. (2009). Expression profile of HIN200 in leukocytes and renal biopsy of SLE patients by real-time RT-PCR. Lupus *18*, 1066–1072. https://doi.org/10.1177/0961203309106699.
20. Cao, T., Shao, S., Li, B., Jin, L., Lei, J., Qiao, H., and Wang, G. (2016). Up-regulation of Interferon-inducible protein 16 contributes to psoriasis by modulating chemokine production in keratinocytes. Sci. Rep. *6*, 25381. https://doi.org/10.1038/srep25381.
21. Alunno, A., Caneparo, V., Bistoni, O., Caterbi, S., Terenzi, R., Gariglio, M., Bartoloni, E., Manzo, A., Landolfo, S., and Gerli, R. (2016). Circulating interferon-inducible protein IFI16 correlates with clinical and serological features in rheumatoid arthritis. Arthritis Care Res. *68*, 440–445. https://doi.org/10.1002/acr.22695.
22. Vanhove, W., Peeters, P.M., Staelens, D., Schraenen, A., Van der Goten, J., Cleynen, I., De Schepper, S., Van Lommel, L., Reynaert, N.L., Schuit, F., et al. (2015). Strong upregulation of AIM2 and IFI16 inflammasomes in the mucosa of patients with active inflammatory bowel disease. Inflamm. Bowel Dis. *21*, 2673–2682. https://doi.org/10.1097/MIB.0000000000000535.
23. Ma, C., Li, S., Hu, Y., Ma, Y., Wu, Y., Wu, C., Liu, X., Wang, B., Hu, G., Zhou, J., and Yang, S. (2021). AIM2 controls microglial inflammation to prevent experimental autoimmune encephalomyelitis. J. Exp. Med. *218*, e20201796. https://doi.org/10.1084/jem.20201796.
24. Chou, W.C., Guo, Z., Guo, H., Chen, L., Zhang, G., Liang, K., Xie, L., Tan, X., Gibson, S.A., Rampanelli, E., et al. (2021). AIM2 in regulatory T cells restrains autoimmune diseases. Nature *591*, 300–305. https://doi.org/10.1038/s41586-021-03231-w.
25. Yi, Y.S., Jian, J., Gonzalez-Gugel, E., Shi, Y.X., Tian, Q., Fu, W., Hettinghouse, A., Song, W., Liu, R., He, M., et al. (2018). p204 is required for canonical lipopolysaccharide-induced TLR4 signaling in mice. EBioMedicine *29*, 78–91. https://doi.org/10.1016/j.ebiom.2018.02.012.
26. Fan, X., Jiang, J., Zhao, D., Chen, F., Ma, H., Smith, P., Unterholzner, L., Xiao, T.S., and Jin, T. (2021). Structural mechanism of DNA recognition by the p204 HIN domain. Nucleic Acids Res. *49*, 2959–2972. https://doi.org/10.1093/nar/gkab076.
27. Jin, T., Perry, A., Jiang, J., Smith, P., Curry, J.A., Unterholzner, L., Jiang, Z., Horvath, G., Rathinam, V.A., Johnstone, R.W., et al. (2012). Structures of the HIN domain:DNA complexes reveal ligand binding and activation mechanisms of the AIM2 inflammasome and IFI16 receptor. Immunity *36*, 561–571. https://doi.org/10.1016/j.immuni.2012.02.014.
28. Lum, K.K., Howard, T.R., Pan, C., and Cristea, I.M. (2019). Charge-mediated pyrin oligomerization nucleates antiviral IFI16 sensing of herpesvirus DNA. mBio *10*, e01428-19. https://doi.org/10.1128/mBio.01428-19.

29. Au, W.C., Moore, P.A., Lowther, W., Juang, Y.T., and Pitha, P.M. (1995). Identification of a member of the interferon regulatory factor family that binds to the interferon-stimulated response element and activates expression of interferon-induced genes. Proc. Natl. Acad. Sci. USA *92*, 11657–11661. https://doi.org/10.1073/pnas.92.25.11657.

30. Kuehner, J.N., Pearson, E.L., and Moore, C. (2011). Unravelling the means to an end: RNA polymerase II transcription termination. Nat. Rev. Mol. Cell Biol. *12*, 283–294. https://doi.org/10.1038/nrm3098.

31. Ning, S., Pagano, J.S., and Barber, G.N. (2011). IRF7: activation, regulation, modification and function. Genes Immun. *12*, 399–414. https://doi.org/10.1038/gene.2011.21.

32. Holt, K.E., Wertheim, H., Zadoks, R.N., Baker, S., Whitehouse, C.A., Dance, D., Jenney, A., Connor, T.R., Hsu, L.Y., Severin, J., et al. (2015). Genomic analysis of diversity, population structure, virulence, and antimicrobial resistance in Klebsiella pneumoniae, an urgent threat to public health. Proc. Natl. Acad. Sci. USA *112*, E3574–E3581. https://doi.org/10.1073/pnas.1501049112.

33. Lery, L.M.S., Frangeul, L., Tomas, A., Passet, V., Almeida, A.S., Bialek-Davenet, S., Barbe, V., Bengoechea, J.A., Sansonetti, P., Brisse, S., and Tournebize, R. (2014). Comparative analysis of Klebsiella pneumoniae genomes identifies a phospholipase D family protein as a novel virulence factor. BMC Biol. *12*, 41. https://doi.org/10.1186/1741-7007-12-41.

34. Dumigan, A., Cappa, O., Morris, B., Sá Pessoa, J., Calderon-Gonzalez, R., Mills, G., Lancaster, R., Simpson, D., Kissenpfennig, A., and Bengoechea, J.A. (2022). In vivo single-cell transcriptomics reveal Klebsiella pneumoniae skews lung macrophages to promote infection. EMBO Mol. Med. *14*, e16888. https://doi.org/10.15252/emmm.202216888.

35. Cano, V., March, C., Insua, J.L., Aguiló, N., Llobet, E., Moranta, D., Regueiro, V., Brennan, G.P., Millán-Lou, M.I., Martín, C., et al. (2015). Klebsiella pneumoniae survives within macrophages by avoiding delivery to lysosomes. Cell Microbiol. *17*, 1537–1560. https://doi.org/10.1111/cmi.12466.

36. Hertel, L., Rolle, S., De Andrea, M., Azzimonti, B., Osello, R., Gribaudo, G., Gariglio, M., and Landolfo, S. (2000). The retinoblastoma protein is an essential mediator that links the interferon-inducible 204 gene to cell-cycle regulation. Oncogene *19*, 3598–3608. https://doi.org/10.1038/sj.onc.1203697.

37. Liao, J.C.C., Lam, R., Brazda, V., Duan, S., Ravichandran, M., Ma, J., Xiao, T., Tempel, W., Zuo, X., Wang, Y.X., et al. (2011). Interferon-inducible protein 16: insight into the interaction with tumor suppressor p53. Structure *19*, 418–429. https://doi.org/10.1016/j.str.2010.12.015.

38. Hoebe, K., Du, X., Georgel, P., Janssen, E., Tabeta, K., Kim, S.O., Goode, J., Lin, P., Mann, N., Mudd, S., et al. (2003). Identification of Lps2 as a key transducer of MyD88-independent TIR signalling. Nature *424*, 743–748.

39. Kim, H., Erickson, B., Luo, W., Seward, D., Graber, J.H., Pollock, D.D., Megee, P.C., and Bentley, D.L. (2010). Gene-specific RNA polymerase II phosphorylation and the CTD code. Nat. Struct. Mol. Biol. *17*, 1279–1286. https://doi.org/10.1038/nsmb.1913.

40. Bosso, M., Prelli Bozzo, C., Hotter, D., Volcic, M., Stürzel, C.M., Rammelt, A., Ni, Y., Urban, S., Becker, M., Schelhaas, M., et al. (2020). Nuclear PYHIN proteins target the host transcription factor Sp1 thereby restricting HIV-1 in human macrophages and CD4+ T cells. PLoS Pathog. *16*, e1008752. https://doi.org/10.1371/journal.ppat.1008752.

41. Xie, J., Briggs, J.A., and Briggs, R.C. (1998). Human hematopoietic cell specific nuclear protein MNDA interacts with the multifunctional transcription factor YY1 and stimulates YY1 DNA binding. J. Cell. Biochem. *70*, 489–506.

42. McGinley, A.M., Sutton, C.E., Edwards, S.C., Leane, C.M., DeCourcey, J., Teijeiro, A., Hamilton, J.A., Boon, L., Djouder, N., and Mills, K.H.G. (2020). Interleukin-17A serves a priming role in autoimmunity by recruiting IL-1beta-producing myeloid cells that promote pathogenic T cells. Immunity *52*, 342–356.e6. https://doi.org/10.1016/j.immuni.2020.01.002.

43. Chen, W., Yu, S.X., Zhou, F.H., Zhang, X.J., Gao, W.Y., Li, K.Y., Liu, Z.Z., Han, W.Y., and Yang, Y.J. (2019). DNA sensor IFI204 contributes to host defense against Staphylococcus aureus infection in mice. Front. Immunol. *10*, 474. https://doi.org/10.3389/fimmu.2019.00474.

44. Jaffray, E., Wood, K.M., and Hay, R.T. (1995). Domain organization of I kappa B alpha and sites of interaction with NF-kappa B p65. Mol. Cell Biol. *15*, 2166–2172. https://doi.org/10.1128/MCB.15.4.2166.

45. Nassif, X., Fournier, J.M., Arondel, J., and Sansonetti, P.J. (1989). Mucoid phenotype of Klebsiella pneumoniae is a plasmid-encoded virulence factor. Infect. Immun. *57*, 546–552. https://doi.org/10.1128/iai.57.2.546-552.1989.

46. Mulcahy, M.E., O'Brien, E.C., O'Keeffe, K.M., Vozza, E.G., Leddy, N., and McLoughlin, R.M. (2020). Manipulation of autophagy and apoptosis facilitates intracellular survival of Staphylococcus aureus in human neutrophils. Front. Immunol. *11*, 565545. https://doi.org/10.3389/fimmu.2020.565545.

47. Sato, M., Suemori, H., Hata, N., Asagiri, M., Ogasawara, K., Nakao, K., Nakaya, T., Katsuki, M., Noguchi, S., Tanaka, N., and Taniguchi, T. (2000). Distinct and essential roles of transcription factors IRF-3 and IRF-7 in response to viruses for IFN-alpha/beta gene induction. Immunity *13*, 539–548. https://doi.org/10.1016/s1074-7613(00)00053-4.

48. Honda, K., Yanai, H., Negishi, H., Asagiri, M., Sato, M., Mizutani, T., Shimada, N., Ohba, Y., Takaoka, A., Yoshida, N., and Taniguchi, T. (2005). IRF-7 is the master regulator of type-I interferon-dependent immune responses. Nature *434*, 772–777. https://doi.org/10.1038/nature03464.

49. Takayanagi, H., Kim, S., Matsuo, K., Suzuki, H., Suzuki, T., Sato, K., Yokochi, T., Oda, H., Nakamura, K., Ida, N., et al. (2002). RANKL maintains bone homeostasis through c-Fos-dependent induction of interferon-beta. Nature *416*, 744–749. https://doi.org/10.1038/416744a.

50. Fitzgerald, K.A., McWhirter, S.M., Faia, K.L., Rowe, D.C., Latz, E., Golenbock, D.T., Coyle, A.J., Liao, S.M., and Maniatis, T. (2003). IKKepsilon and TBK1 are essential components of the IRF3 signaling pathway. Nat. Immunol. *4*, 491–496. https://doi.org/10.1038/ni921.

51. Lin, R., Heylbroeck, C., Pitha, P.M., and Hiscott, J. (1998). Virus-dependent phosphorylation of the IRF-3 transcription factor regulates nuclear translocation, transactivation potential, and proteasome-mediated degradation. Mol. Cell Biol. *18*, 2986–2996. https://doi.org/10.1128/MCB.18.5.2986.

52. Lin, R., Mamane, Y., and Hiscott, J. (2000). Multiple regulatory domains control IRF-7 activity in response to virus infection. J. Biol. Chem. *275*, 34320–34327. https://doi.org/10.1074/jbc.M002814200.

53. Brady, G., Haas, D.A., Farrell, P.J., Pichlmair, A., and Bowie, A.G. (2017). Molluscum contagiosum virus protein MC005 inhibits NF-kappaB activation by targeting NEMO-regulated IkappaB kinase activation. J. Virol. *91*, e00545-17. https://doi.org/10.1128/JVI.00545-17.

54. Radons, J., Gabler, S., Wesche, H., Korherr, C., Hofmeister, R., and Falk, W. (2002). Identification of essential regions in the cytoplasmic tail of interleukin-1 receptor accessory protein critical for interleukin-1 signaling. J. Biol. Chem. *277*, 16456–16463. https://doi.org/10.1074/jbc.M201000200.

55. Kuprash, D.V., Udalova, I.A., Turetskaya, R.L., Kwiatkowski, D., Rice, N.R., and Nedospasov, S.A. (1999). Similarities and differences between human and murine TNF promoters in their response to lipopolysaccharide. J. Immunol. *162*, 4045–4052.

56. Seshadri, S., Kannan, Y., Mitra, S., Parker-Barnes, J., and Wewers, M.D. (2009). MAIL regulates human monocyte IL-6 production. J. Immunol. *183*, 5358–5368. https://doi.org/10.4049/jimmunol.0802736.

57. Stewart, S.A., Dykxhoorn, D.M., Palliser, D., Mizuno, H., Yu, E.Y., An, D.S., Sabatini, D.M., Chen, I.S.Y., Hahn, W.C., Sharp, P.A., et al. (2003). Lentivirus-delivered stable gene silencing by RNAi in primary cells. RNA *9*, 493–501. https://doi.org/10.1261/rna.2192803.

58. Zhang, X., Goncalves, R., and Mosser, D.M. (2008). The isolation and characterization of murine macrophages. Curr. Protoc. Immunol. *Chapter 14*, Unit 14. https://doi.org/10.1002/0471142735.im1401s83.

59. Hornung, V., Bauernfeind, F., Halle, A., Samstad, E.O., Kono, H., Rock, K.L., Fitzgerald, K.A., and Latz, E. (2008). Silica crystals and aluminum salts activate the NALP3 inflammasome through phagosomal destabilization. Nat. Immunol. *9*, 847–856. https://doi.org/10.1038/ni.1631.

60. Pader, V., James, E.H., Painter, K.L., Wigneshweraraj, S., and Edwards, A.M. (2014). The Agr quorum-sensing system regulates fibronectin binding but not hemolysis in the absence of a functional electron transport chain. Infect. Immun. *82*, 4337–4347. https://doi.org/10.1128/IAI.02254-14.

61. Ivin, M., Dumigan, A., de Vasconcelos, F.N., Ebner, F., Borroni, M., Kavirayani, A., Przybyszewska, K.N., Ingram, R.J., Lienenklaus, S., Kalinke, U., et al. (2017). Natural killer cell-intrinsic type I IFN signaling controls Klebsiella pneumoniae growth during lung infection. PLoS Pathog. *13*, e1006696. https://doi.org/10.1371/journal.ppat.1006696.

STAR★METHODS

KEY RESOURCES TABLE

REAGENT or RESOURCE	SOURCE	IDENTIFIER
Antibodies		
Acetylated H3	Millipore	Cat#06-599; RRID: AB_2115283
FC block	BioLegend	Cat#101302; RRID: AB_312801
Ifi207-A764	This paper (Storkbio)	N/A
Ifi207-R196-A764 serum	This paper (Storkbio)	N/A
Ifi207-R230-A764 serum	This paper (Storkbio)	N/A
IFNβ capture antibody	Santa Cruz	Cat#SC-57201; RRID: AB_2122911
IFNβ detection antibody	PBL InterferonSource	Cat#32400-1; RRID: AB_387872
IFNAR1 blocking antibody	Invitrogen	Cat#16-5945; RRID: AB_1210687
IkBα	Gift from R. T. Hay, University of Dundee, UK Jaffray et al.[44]	N/A
IRDye 680RD Goat α-Mouse IgG	Li-Cor	Cat#926-68070; RRID: AB_10956588
IRDye 800CW Goat α-Rabbit IgG	Li-Cor	Cat#926-32211; RRID: AB_621843
IRF3	Invitrogen	Cat#51-3200; RRID: AB_2533904
Non-specific IgG from rabbit serum	Sigma	Cat#NI01; RRID: AB_490574
p38	Cell Signaling	Cat#9212; RRID: AB_330713
p65	Santa Cruz	Cat#sc-372; RRID: AB_632037
phospho-IRF3	Cell Signaling	Cat#4947; RRID: AB_823547
phospho-p38	Cell Signaling	Cat#4511; RRID: AB_2139682
phospho-p65	Cell Signaling	Cat#3031; RRID: AB_330559
Phosphor-Akt	Cell Signaling	Cat#9271; RRID: AB_329825
PI-R196 pre-immune serum	This paper (Storkbio)	N/A
PI-R230 pre-immune serum	This paper (Storkbio)	N/A
RNA pol II	Santa Cruz	Cat#sc-899; RRID: AB_632359
S2p-RNA pol II	Abcam	Cat#ab5095; RRID: AB_304749
S5p-RNA pol II	Abcam	Cat#ab5131; RRID: AB_449369
Tubulin	Sigma-Aldrich	Cat#T6074; RRID: AB_477582
αCD11c-APC	TONBO Biosciences	Cat#20-0114; RRID: AB_2621557
αCD19-FITC	BioLegend	Cat#152404; RRID: AB_2629813
αF4/80-PE	TONBO Biosciences	Cat#50-4801; RRID: AB_2621795
αFlag	Merck	Cat#F1804; RRID: AB_262044
αHA	BioLegend	Cat# 901514; RRID: AB_2565336
αHA-Alexa594	Invitrogen	Cat#21288; RRID: AB_1500205
αMouse HRP	Bio-Rad	Cat#170-6516; RRID: AB_11125547
αMouse-Alexa647	BioLegend	Cat#123122; RRID: AB_893480
αRabbit HRP	Bio-Rad	Cat#170-6515; RRID: AB_11125142
αRabbit-Alexa488	BioLegend	Cat#406416; RRID: AB_2563203
αTCRb-BV605	BioLegend	Cat#109241; RRID: AB_2629563
β-actin	Merck	Cat#A5316; RRID: AB_476743
Bacterial and virus strains		
Klebsiella Pneumoniae strain: Kp52145	Institut Pasteur, France Lery et al. ; Nassif et al.[33,45]	N/A
Staphylococcus aureus strain: USA300 LAC	Trinity College Dublin Mulcahy et al.; Jaffray et al.[44,46]	N/A

(*Continued on next page*)

Continued

REAGENT or RESOURCE	SOURCE	IDENTIFIER
Chemicals, peptides, and recombinant proteins		
Ifi207 immunisation peptide: (NH2)CSRLQ SSQKPLEAHLDLKMSPSSSRSP(CONH2)	This paper (Storkbio)	N/A
Freund's adjuvant (CFA)	Chondrex	Cat#7008
LPS	Enzo Life Sciences	Cat#581-010-L002
$MOG_{35–55}$	GeneScript	Cat#RP10245
mouse recombinant IFNβ	Pbl Assay Science	Cat#12410-1
Pam3CSK4	InvivoGen	Cat#tlrl-pms
pertussis toxin (PT)	Kaketsucken	N/A
poly(I:C) HMW	InvivoGen	Cat#tlrl-pic
Critical commercial assays		
Mouse CCL5/RANTES DuoSet Elisa	R&D Systems	Cat#DY478
Mouse Cxcl10/IP10 DuoSet Elisa	R&D Systems	Cat#DY466
Mouse IL6 DuoSet Elisa	R&D Systems	Cat#DY406
Mouse TNF-alpha Duoset Elisa	R&D Systems	Cat#DY410
Experimental models: Cell lines		
293/TLR4-MD2-CD14	InvivoGen	Cat#293-htlr4md2cd14
HEK293T	ECACC	ECACC 12022001
HeLa	ECACC	ECACC 93021013
Immortalised BMDMs: *Irf3*$^{-/-}$ and *Irf7*$^{-/-}$	Generated from mice gifted by Prof. Tadatsugu Taniguchi,University of Tokyo, Japan Sato et al.; Honda et al.[47,48]	N/A
Immortalised BMDMs: WT and *Ifi207*$^{-/-}$	This paper	N/A
J774	ECACC	ECACC 91051511
RAW264.7	ECACC	ECACC 91062702
Experimental models: Organisms/strains		
mouse wild type: C57BL/6J	The Jackson Laboratory	Cat#000664
mouse *Ifi207*$^{-/-}$: C57BL/6J-Ifi207^{em1Wor}	This paper	N/A
Oligonucleotides		
Alcds1gR199r gRNA: CAGTTCACC CAATCCAGCATCGG	This paper	N/A
Alcds2gR151f gRNA: AAGAGACTTC CACAGCTCAGGGG	This paper	N/A
Alcds2gR197r gRNA: TCTTTCAGATG TTAGCATGTGG	This paper	N/A
Alcds1gR198r gRNA: AGTTCACCCA ATCCAGCATCGGG	This paper	N/A
pLKO.1 sequencing primer: AAGGCT GTTAGAGAGATAATTGGA	Addgene protocols	N/A
VV70mer	Previously described Unterholzner et al.[6]	N/A
qPCR primers: see Table S1	This paper	N/A
Ifi207 genotyping primers – see Table S2	This paper	N/A
Ifi207 and its truncations cloning primers – see Table S2	This paper	N/A
Recombinant DNA		
m*Ifnβ*-reporter (p125-Mu-luc)	Gift from Prof. Tadatsugu Taniguchi, University of Tokyo, Japan Takayanagi et al.[49]	N/A
pcDNA3-Flag-IKKε	Previously described Fitzgerald et al.[50]	N/A

(*Continued on next page*)

Continued

REAGENT or RESOURCE	SOURCE	IDENTIFIER
pcDNA3-Flag-TBK	Previously described Fitzgerald et al.[50]	N/A
pCMV-HA	Clontech	Cat#631604
pCMV-HA-Ifi207	This paper	N/A
pCMV-HA-Ifi207ΔHIN	This paper	N/A
pCMV-HA-Ifi207ΔPyr	This paper	N/A
pCMV-HA-Ifi207ΔPyrHIN	This paper	N/A
pCMV-HA-Pyr207	This paper	N/A
pCR4-TOPO-Ifi207	ImaGenes	IRCKp5014A0215Q
pMSCV-PIG-IFI205-HA	Previously described Ghosh et al.[14]	N/A
pFlag-IRF3-5D	Gift from Prof. John Hiscott, Pasteur Laboratories, Rome, Italy Lin et al.[51]	N/A
pFlag-IRF7	Gift from Prof. John Hiscott, Pasteur Laboratories, Rome, Italy Lin et al.[52]	N/A
pFlag-IRF7-4D	Gift from Prof. John Hiscott, Pasteur Laboratories, Rome, Italy Lin et al.[52]	N/A
MyD88-Myc	Previously described Brady et al.[53]	N/A
pGL3–5xNFkB	Gift from Dr Robert Hofmeister, Universität Regensburg, Germany Radons et al.[54]	N/A
pGL3-*Asc*-luc (−2000)	Previously described Gosh et al.[14]	N/A
pGL3-h*TNF*(-1173)	Gift from Prof. Irina Udalova, University of Oxford, UK kuprash et al.[55]	N/A
pGL3-m*Tnf*(-1260)	Gift from Dr D Kuprash, EIMB, Moscow, Russia kuprash et al.[55]	N/A
phRL-TK reporter	Promega	Cat#E6241
pIL6-luc651	Gift from Prof. Mark Wewers, The Ohio State University, Columbus, USA Seshadri et al.[56]	N/A
pISRE-luc	Agilent	Cat#219089
pLKO.1- Ctrl shRNA lentiviral vector, target sequence:CAACAAGATGAAG AGCACCAA	This paper	N/A
pLKO.1 puro lentiviral vector	Addgene Stewart et al.[57]	Addgene#8453
pLKO.1-Ifi204shRNA lentiviral vector, target sequence: ACCTGAATGCCA ATGATATTT	This paper	N/A
pLKO.1-Ifi207shRNA lentiviral vector, target sequence: GGGCTTTCTTATA TGCTTTAC	This paper	N/A
pLKO.1-Ifi207shRNA#2 lentiviral vector, target sequence: AACTCTATCAACAA CATCTAG	This paper	N/A
pMD2.G lentiviral envelope vector	Addgene (Trono D., unpublished)	Addgene#12259
psPAX2 lentiviral packaging vector	Addgene (Trono D., unpublished)	Addgene#12260
Software and algorithms		
Ensmbl genome browser	Ensmbl	https://www.ensembl.org/index.html
GraphPad Prism 9	GraphPad	ver. 9.3.1
Laica Application Suite X	Laica	ver. 3.7.4
Odyssey Software	Li-Cor	ver. 3.0.16
shRNA hairpin design software	Broad Institute	https://portals.broadinstitute.org/gpp/public/

(*Continued on next page*)

Continued

REAGENT or RESOURCE	SOURCE	IDENTIFIER
ImageJ	Wayne Rasband and contributors	1.53k
Studio Lite	Li-Cor	Ver 4.0

RESOURCE AVAILABILITY

Lead contact

Further information and requests for resources and reagents should be directed to and will be fulfilled by the lead contact, Andrew G. Bowie (agbowie@tcd.ie).

Materials availability

All unique reagents generated in this study are available from the lead contact with a completed Materials Transfer Agreement.

Data and code availability

- All data reported in this paper will be shared by the lead contact upon request.
- This paper does not report any original code.
- Any additional information required to reanalyze the data reported in this paper is available from the lead contact upon request.

EXPERIMENTAL MODEL AND SUBJECT DETAILS

Animal model

To study the role of IFI207 *in vivo* and *in vitro*, C57BL/6J-Ifi207^{em1Wor} mice (herein referred to as *Ifi207*$^{-/-}$) were generated at UMass Chan Medical School on a C57BL/6J background using CRISPR/Cas9 technology. This generated a deletion spanning Exons 2 and 3, resulting in the frameshift of 177nt into the *Ifi207* sequence and introduction of a new early STOP codon within Exon 4 (see Figure 3A for more detail). A mix of adult (8–12 week old) male and female wild type and *Ifi207*$^{-/-}$ mice were used for *in vivo* experiments, and for isolation of bone marrow to generate primary cells (BMDMs and BMDCs) for *in vitro* studies. All animal experiments performed at TBSI (EAE and intranasal *S. aureus* infections) were in compliance with the Irish Health Products Regulatory Authority (HPRA), the competent authority in Ireland and approved by Trinity College Animal Research Ethics Committee. Intranasal *Klebsiella* infections were performed at Queens University Belfast and approved by the Queen's University Belfast Animal Welfare and Ethical Review Body (AWERB). That work was conducted in accordance with the UK Home Office regulations under project licence PPL2910.

Primary cells

Primary cells were differentiated from bone marrow cells isolated from wild type and *Ifi207*$^{-/-}$ mice. Primary BMDMs were differentiated in DMEM supplemented with 10% (v/v) FCS, 1% (v/v) Penicillin-Streptomycin and 15–20% (v/v) L929 supernatant as a source of M-CSF. On days 7–9 cells were seeded for experiments. Primary DC2 BMDCs were differentiated from bone marrow cells in complete RPMI medium supplemented with 10% (v/v) FCS, 1% (v/v) Penicillin-Streptomycin and 20 ng/mL of GM-CSF. On day 10 cells were seeded for experiments in medium supplemented with 10 ng/mL of GM-CSF. Primary DC1 BMDCs were differentiated from bone marrow cells in complete RPMI medium supplemented with 10% (v/v) FCS, 1% (v/v) Penicillin-Streptomycin, 0.5% (v/v) β-mercaptoethanol (Gibco), 52.5 ng/mL Flt3L and 4 ng/mL GM-CSF. Cells were seeded for experiments on day 15. Peritoneal macrophages were isolated from WT and *Ifi207*$^{-/-}$ mice as described before.[58] Mice were injected intraperitoneally with 3% Brewer thioglycolate medium and cells were obtained from peritoneal lavage 3–4 days post injection. Peritoneal macrophages were then cultured and stimulated in DMEM medium supplemented with 10% FCS (v/v) and 1% (v/v) Penicillin-Streptomycin.

Cell lines

Raw264.7, J774, HEK293T and HeLa cells were purchased from the European Collection of Authenticated Cell Cultures (ECACC). 293/TLR4-MD2-CD14 cells were from InvivoGen. RAW264.7 and J774 cells were cultured in DMEM, supplemented with 10% FCS (v/v) and 10 mg/mL Ciprofloxacin (Sigma). HeLa and HEK293T cells were cultured in DMEM, supplemented with 10% FCS (v/v) and 100 μg/ml Normocin (InvivoGen). 293/TLR4-MD2-CD14 cells were cultured in DMEM medium supplemented with 10% FCS (v/v), 10 μg/ml Blasticidin (InvivoGen), 50 μg/ml of HygroGold (InvivoGen) and 100 μg/ml Normocin (InvivoGen). All cells were maintained at 37°C with 5% CO2. Immortalized wild type (WT) and *Ifi207*$^{-/-}$ BMDMs were generated with J2 recombinant retrovirus carrying v-myc and v-raf oncogenes as previously described[59] and grown in DMEM, supplemented with 10% FCS (v/v) and 100 μg/ml of Normocin. *Irf3*$^{-/-}$ and *Irf7*$^{-/-}$ BMDMs were immortalised from mice kindly provided by Prof. Tadatsugu Taniguchi (Department of Immunology, Faculty of Medicine and Graduate School of Medicine, University of Tokyo, Japan).[47,48]

Bacterial strains

Klebsiella pneumoniae strain Kp52145 (received from Institut Pasteur, France) is a clinical isolate (serotype O1:K2) previously described[33,45] and was cultured in LB medium at 37°C. *Staphylococcus aureus* strain USA300 LAC have been described previously.[46,60] *S. aureus* strain was streaked from frozen stocks onto TSA plates and grown at 37°C for 24 h. Both bacterial strains were used for *in vitro* and *in vivo* studies.

METHOD DETAILS

Cell treatments with stimulants and bacteria

LPS (Enzo), Pam3CSK4 (InvivoGen) and recombinant IFNβ (Pbl Assay Science) were used at the concentrations indicated in figure legends. The vaccinia virus 70 bp dsDNA oligonucleotide (VV70mer) was synthesised by Integrated DNA technologies (IDT) and has been described previously.[6] Transfection of RAW264.7 and J774s with VV70mer or poly(I:C) (InvivoGen) and HeLa cells with plasmids expressing IFI207-Ha and its truncations was performed using Lipofectamine 2000 (InvitroGen) following the manufacturer's recommended protocol. Transfection of HEK293T and 293/TLR4-MD2-CD14 cells with plasmid DNA for Reporter Gene Assays were performed using GeneJuice (Merck) following the manufacturer's recommended protocol.

For *K. pneumoniae* infection of cells, the overnight bacterial cultures were refreshed 1/10 into a new tube containing 4.5 ml of fresh LB. After 2.5 h at 37°C, bacteria were pelleted (2500× g, 20 min, 22°C), resuspended in PBS and adjusted to an optical density of 1.0 at 600 nm (5 x 10^8 CFU/ml). Infections were performed using a multiplicity of infection (MOI) of 100 bacteria per cell in a 1 ml volume. Synchronization of the infection was performed by centrifugation (200 x g for 5 min). For incubation times longer than 30 min, cells were washed and 1 ml of fresh medium containing gentamycin (100 μg/ml) was added to the wells to kill extracellular bacteria. Medium containing gentamycin was kept until the end of the experiment. Infections were performed one day after seeding the cells in the same medium used to maintain the cell line without antibiotics. Infected cells were incubated at 37°C in a humidified 5% CO2 incubator.

S. aureus suspensions were prepared in sterile PBS and the OD at 600 nm adjusted to the desired equivalent CFU/ml. Cells were seeded in 24-well plates (5x10^6 /well) approximately 16 h before infection. *S. aureus* USA 300 LAC MOI 100 was added to the cells for 1 h upon which media was removed. Cells were then treated with gentamycin (200ug/ml) for 1 h upon which media was refreshed. RNA analysis was assessed 3, 6 and 24 h post gentamycin treatment.

Bacterial adhesion, phagocytosis and survival

Intracellular survival experiments were carried out as previously described with minor modifications.[34] iBMDMs were seeded in 12- or 24-well plates (5x10^6 /well) approximately 16 h before infection. Cells were infected with *S. aureus* USA300 LAC at MOI 100 or *K. pneumoniae* Kp52145 at MOI 70. To enumerate the number of bacteria adhered to macrophages, after 30 min of contact, cells were washed twice with PBS and were lysed in either 150μL of 0.1% (wt/vol) triton (Sigma) in PBS for 10 min at 37°C (*S. aureus*) or 300μl of 0.05% saponin (Sigma) in PBS for 5 min at 37°C (*K. pneumoniae*). Serial dilutions were plated and the following day bacterial CFUs were counted. Results are expressed as CFU/ml. To determine the number of bacteria phagocytosed by the cells, after 30 min of contact, cells were washed once with PBS and fresh medium containing gentamycin (100-200 μg/mL) was added to the wells to kill the extracellular bacteria. After 30 min, cells were washed with PBS, and lysed. Serial dilutions were plated and the following day bacterial CFUs were counted. Results are expressed as CFU/ml. To assess intracellular survival, cells were washed with PBS 4-5 h after the addition of gentamycin and then lysed. Serial dilutions were plated and the following day bacterial CFUs were counted. Results are expressed as percent of survival calculated as CFUs in *Ifi207*$^{-/-}$ cells at 4-5 h versus 30min and normalised to the results obtained for WT macrophages set to 100%.

Generation of PYHIN shRNA-expressing cells

RAW264.7 and J774 shRNA expressing cells were created using pLKO.1 lentiviral vector (Addgene#8453)[57] and following the recommended protocols from AddGene (https://www.addgene.org/protocols/plko/). ShRNA targets and their sequences were: 3'UTR region of *Ifi207* mRNA (Ifi207 shRNA: GGGCTTTCTTATATGCTTTAC); coding region of *Ifi207* mRNA (Ifi207 shRNA#2: AACTC TATCAACAACATCTAG); 3'UTR region of *Ifi204* mRNA (Ifi204 shRNA: ACCTGAATGCCAATGATATTT); non-targeting control shRNA (Ctrl shRNA: CAACAAGATGAAGAGCACCAA). These were cloned into the pLKO.1 lentiviral expression vector using AgeI and EcoRI restriction enzymes. Successful cloning was confirmed by Sanger sequencing using pLKO.1 sequencing primer: 5'-AAGGCTGTTA GAGAGATAATTGGA-3'. Lentiviruses containing shRNA oligos were then created in HEK293T cells. Cells were transfected using GeneJuice (Merck) with combination of corresponding pLKO.1 shRNA expression plasmid together with the lentiviral packaging (psPAX2, Addgene#12260) and envelope (pMD2.G, Addgene#12259) plasmids. Supernatants containing shRNA carrying lentiviruses were harvested 48 and 72 h post transfection, centrifuged (5 min, 2000x g), filtered through sterile 0,45μm filters and used for generation of shRNA expressing cells. ShRNA lentivirus containing medium, supplemented with 8 μg/ml of Polybrene (Sigma), was added to RAW264.7 or J774 cells and cells were incubated overnight at 37°C in a humidified 5% CO2 incubator. Cell medium was then replaced by complete DMEM supplemented with 10% (v/v) of FCS and 10 mg/mL Ciprofloxacin. Following the 24-48 h incubation, cells were moved to selection medium composed of complete DMEM additionally supplemented with 5μg/ml of Puromycin (Sigma). After the initial selection, cells were cultured in complete DMEM medium supplemented with 1 μg/ml of Puromycin.

Cloning of IFI207 and its truncations

pCR4-TOPO plasmid containing the *Ifi207* sequence (AccNo.: BC150711), originating from a mouse brain and spleen pooled cDNA library, was purchased from ImaGenes (Clone: IRCKp5014A0215Q). It was then amplified using PfuTurbo polymerase (Agilent) using primers: IFI207-HA-Forw, IFI207-HA-Rev and cloned into the pCMV-HA (Clontech) plasmid using SalI and NotI restriction enzymes (New England Biolabs). Newly created pCMV-HA-IFI207 plasmid was then used to create a range of IFI207 truncations using primer combinations: IFI207ΔPyr (IFI207dPyr-Forwand IFI207-HA-Rev), IFI207ΔHIN (IFI207-HA-Forw and IFI207dHIN-Rev), IFI207ΔPyrHIN (IFI207dPyr-Forw and IFI207dHIN-Rev), Pyr207 (IFI207-HA-Forw and Pyr207-Rev). *Ifi207* cloning primer sequences can be found in Table S2. They were amplified using KOD polymerase (Merck) and cloned into the pCMV-HA plasmid using SalI and NotI restriction enzymes. Successful cloning of all created plasmids was then confirmed by sequencing and the protein expression was confirmed in transfected HEK293T cells by immunoblot using anti-HA primary antibody.

Generation of IFI207 antibody

A764 rabbit polyclonal antibody was raised against IFI207 peptide (NH2)CSRLQSSQKPLEAHLDLKMSPSSSRSP(CONH2). The peptide was chosen based on the IFI207 amino acid sequence (NP_001191839.1) and considering its antigenicity and surface probability indexes as well as its lack of cross-reactivity with the majority of other murine PYHIN family members. Both the peptide and the antibody were produced by Storkbio. Antibody was obtained by immunization of two rabbits (R196 & R230) and both pre-immune (R196 A764 PI and R230 A764 PI) and final sera (R196 A764 and R230 A764) were received. Epitope-specific purification was also performed to obtain a purified A764 antibody. Due to some overlap of the peptide sequence with the sequences of IFI203 isoforms, some cross-reactivity with IFI203 is possible. However, due to significant difference in protein sizes between IFI207 and IFI203 as well as very low expression of IFI203 detected in macrophages this had no impact on the usefulness of the antibody in our study.

ELISA for cytokine secretion

Quantification of secreted murine TNFα, IP10 (CXCL10), IL6 and CCL5 was performed using ELISA kits from R&D, namely the Mouse TNF-alpha DuoSet (DY410), Mouse CXCL10/IP10 DuoSet (DY466), Mouse IL6 Duoset (DY406) and the Mouse CCL5/RANTES DuoSet (DY478), following the manufacturer's recommended protocol. Mouse IFNβ production was quantified by ELISA using the in-house protocol. ELISA plates were coated with a monoclonal rat anti-mouse IFNβ capture antibody (Santa Cruz, Cat#SC-57201) in carbonate buffer and a polyclonal rabbit anti-mouse IFNβ (PBL InterferonSource, Cat#32400-1) in blocking solution (10% FCS/PBS) was used as a detection antibody. HRP-conjugated anti-rabbit IgG antibody (Sigma, Cat# RABHRP1) was used for TMB substrate (BD) development. Absorbances for 450 and 620 nm wavelengths were obtained using the Spectramax ELISA plate reader (Molecular Devices) and concentrations were calculated based on standard curve of recombinant murine IFNβ (PBL InterferonSource, Cat#12400-1).

RNA analysis by quantitative RT-PCR

For PAMP stimulated RAW264.7, J774, iBMDMs as well as primary BMDMs, BMDCs and splenocytes, and *S. aureus* infected primary BMDMs, total RNA was extracted from cells using the High Pure RNA Isolation Kit (Roche) according to manufacturer's instructions. Lung tissue from *S. aureus* infected mice was homogenised using TissueLyser (Qiagen) and total RNA was isolated using Trizol reagent (Ambion) following manufacturer's protocol. Reverse transcription with random hexamers (IDT) was done using Moloney murine leukaemia virus reverse transcriptase (MyBio) according to the manufacturer's instructions. mRNA was quantified with PowerUp SYBR Green (Applied Biosystems) using primer pairs targeting genes of interest (for full list see Table S1). RT-PCR was performed using QuantiStudio 3 (Applied Biosystems). Relative mRNA expression was calculated using the comparative CT method, normalizing the gene of interest to the housekeeping gene β-actin.

For *Klebsiella* infected primary BMDMs and lung tissues, total RNA was extracted from the cells in 1 ml of TRIzol reagent (Ambion) according to the manufacturer's instructions. Extracted RNA was treated with DNase I (Roche) and precipitated with sodium acetate (Ambion) and ethanol. RNA was then quantified using a Nanovue Plus spectrophotometer (GE Healthcare Life Sciences). cDNA was generated by reverse transcription of total RNA using M-MLV reverse transcriptase (Invitrogen) and random primers (Invitrogen). Generated cDNA was used as a template for RT-qPCR reaction with KAPA SYBR FAST qPCR kit (Kapa Biosystems) that was performed using a Rotor-Gene Q (Qiagen). Relative quantities of mRNAs were calculated using the comparative CT method, normalizing the gene of interest to the housekeeping gene hypoxanthine phosphoribosyl transferase 1 (hprt).

Immunoblotting

Cells were lysed in the WB sample buffer (10% v/v Glycerol, 10% w/v SDS, 0.1% w/v Bromophenol Blue, 62.5mM Trizma Base,50mM DTT, pH 6.8) and subjected to SDS-PAGE and immunoblotting. Primary antibodies used were as follows: IFI207-A764 (1:1000), IFI207-R196 and IFI207-R230 serum (1:1000), PI-R196 and PI-R230 pre-immune serum (1:1000), β-actin (1:10000, Merck A5316), αHA (1:2000, BioLegend #901514), αFlag (1:5000, Merck #F1804), phospho-IRF3 (1:1000, Cell Signalling #4947), IRF3 (1:1000, Invitrogen #51-3200), phospho-p65 (1:1000, Cell Signalling #3031), p65 (1:1000, Santa Cruz sc-372), IkBα (1:1000, kind gift from R. T. Hay, University of Dundee, UK[44]), phospho-p38 (1:1000, Cell Signalling #4511), p38 (1:1000, Cell Signalling #9212), phospho-AKT (1:1000, Cell Signaling #9271) and Tubulin (1:4000, Sigma-Aldrich #T6074). The next day, membranes were incubated secondary antibodies IRDye 680RD Goat anti-Mouse IgG (1:10000, Li-Cor 926-68070) or IRDye 800CW Goat anti-Rabbit

IgG (1:10000, Li-Cor 926-32211). Blots were visualised using the Odyssey imaging system (Li-Cor Biosciences) and analysed using the Odyssey Software ver. 3.0.16 and Image Studio Lite Ver 4.0 software. For phospho-Akt and Tubulin immunoblots, bands were visualised by incubation with horseradish peroxidase-conjugated goat anti-rabbit antibody (1:5000, Bio-Rad #170-6515) or goat anti-mouse antibody (1:5000, Bio-Rad #170-6516). Protein bands were visualised using chemiluminescence reagents and a G:BOX Chemi XRQ chemiluminescence imager (Syngene).

Co-immunoprecipitation

HEK293T cells, grown in 10 cm dishes, were transfected using GeneJuice (Merck) with combinations of plasmids expressing IFI207-HA (pCMV-HA-IFI207), IRF7-Flag (pFlag-IRF-7, kind gift from Prof. John Hiscott, Pasteur Laboratories, Rome, Italy)[52] and pCMV-HA (Clontech) empty vector for 48h. Cells were lysed in NP-40 lysis buffer (50 mM HEPES pH 7.5, 200 mM NaCl, 1 mM EDTA, 10% (v/v) glycerol, 1 % (v/v) NP-40 containing 10 μl/ml Aprotinin, 1 mM PMSF and 1 mM sodium orthovanadate) and immunoprecipitation using protein G-sepharose beads (Fisher Scientific) and anti-HA antibody (BioLegend #901514) was performed overnight at 4°C. Beads were then washed, precipitated protein complexes were released by boiling in WB sample buffer and co-immunoprecipitation between IFI207-HA and IRF7-Flag was analysed by immunoblot.

Chromatin immunoprecipitation

Cells, grown in 15 cm dishes were stimulated with LPS as specified in figure legends. Following stimulation cells were fixed for 10-15 min at room temperature with 1% (v/v) formaldehyde. Formaldehyde was then quenched with 0.125 M glycine for 10 min. Cells were then washed with ice cold PBS, scraped and centrifuged (1200 g for 5 min at 4°C). Cells were lysed on ice in 1 ml of IP buffer (50 mM Tris-HCl pH 7.5, 150 mM NaCl, 5 mM EDTA, 0.5% NP-40, 1% Triton X-100) with addition of protease inhibitors: 0.1 mM PMSF, 1 mM Na_3VO_4 and 10 μl/ml Aprotinin (Merck). Cell lysates were then centrifuged (16000 g for 1 min at 4°C), supernatant was removed, and pellet was once more reconstituted in 1 ml of IP buffer with inhibitors followed by another centrifugation and reconstitution step. Cell lysates were then sonicated using a Branson Sonifier 250 to shear genomic DNA. Samples were centrifuged (16000 g for 1 min at 4°C) to remove the remaining debris. 50 μl of the sheared gDNA was then kept as INPUT control sample and the rest was divided evenly and mixed with 1-2 μg of appropriate antibody: RNA pol II (Santa Cruz #sc-899), acetylated H3 (Millipore #06-599) or non-specific IgG from rabbit serum (Sigma #NI01) and 30 μl of 50% solution of protein A–Sepharose beads blocked previously with BSA (0.5 mg/ml of beads) and salmon sperm DNA (0.1 mg/ml of beads) to reduce non-specific binding. Following overnight incubation at 4°C the beads were washed 5 times with the IP buffer and bound DNA was eluted with 250 μl of Elution buffer (1% SDS and 0.1 M $NaHCO_3$) at 65 °C for 2 h. The eluent and input were then reverse cross-linked by overnight incubation at 55°C with addition of 0.4 M NaCl followed by treatment with RNAse (Invitrogen) for 1h at 37°C and proteinase K (Qiagen) for 2 h at 55°C. DNA was then extracted using PCR purification kit (Qiagen) and analysed by qPCR using specific primers recognizing the TNF promoter region (mTNF-ChIP-F1and mTNF-ChIP-R1) or a sequence within the last exon of the TNF gene (mTNF-ChIP-F2 and mTNF-ChIP-R2). Primer sequences can be found in Table S1. Data was then normalized to the input DNA and presented as % of input.

Reporter gene assay

Mouse pGL3-m*Tnf*(-1260) and human pGL3-h*TNF*(-1173) TNF-promoter reporters were kind gifts from Dr Dimitry Kuprash (Engelhardt Institute of Molecular Biology (EIMB), Moscow, Russia) and Prof. Irina Udalova (Kennedy Institute of Rheumatology, NDORMS, University of Oxford, UK) respectively.[55] Murine *Ifnβ*–promoter reporter (p125-Mu-luc) was a kind gift from Prof. Tadatsugu Taniguchi (Department of Immunology, Faculty of Medicine and Graduate School of Medicine, University of Tokyo, Japan).[49] Human *IL6*-promoter reporter (pIL6-luc651) was a kind gift from Prof. Mark Wewers (Davis Heart and Lung Research Institute and Pulmonary, Allergy, Critical Care and Sleep Medicine Division, The Ohio State University, Columbus, USA).[56] NFκB-promoter element reporter (pGL3–5xNFkB) was a kind gift from Dr Robert Hofmeister (Klinik und Poliklinik für Innere Medizin I, Universität Regensburg, Germany).[54] ISRE-promoter element reporter (pISRE-luc) was purchased from Agilent (#219089) and mouse *Asc*-promoter reporter (*Asc*-luc) was previously described.[14] HEK293T cells or 293/TLR4-MD2-CD14 cultured in 96 well plates, were transfected using GeneJuice with 60 ng/well of firefly luciferase TNF-promoter reporter plasmid, 20 ng/well of renilla luciferase phRL-TK reporter gene control plasmid (Promega) and the desired amount of plasmids expressing: IFI207, IFI207ΔHIN, Ifi207ΔPYR, IFI207ΔPYRHIN, PYR207, IFI205,[14] TBK1,[50] IKKε,[50] IRF3-5D,[51] IRF7-4D[52] or MyD88[53] (as specified in figure legends). The total amount of the DNA per transfection was kept constant at 230 ng by addition of the pCMV-HA empty vector. When relevant, cells were stimulated with 100 ng/mLl of LPS 24 h post transfection. Cells were lysed 48 h post transfection with Passive Lysis Buffer (PLB; Promega) and assayed for firefly and renilla luciferase activity. The final reporter activity was normalized to the activity of renilla luciferase control within each sample and presented as mean fold induction over reporter gene only control.

Confocal microscopy

HeLa cells, grown on coverslips, were transfected with IFI207 expression plasmids or pCMV-HA empty vector using Lipofectamine 2000 (Invitrogen), following the manufacturer's protocol. 24-48 h post transfection, cells were washed with PBS and fixed on ice for 10 min with 4% paraformaldehyde (PFA). The washing step was repeated, and the cells were permeabilised using 0.5% Triton X-100 (Merck) for 15 min. Following another washing step cells were blocked with 5% w/v BSA in PBS for 1 h in room temperature. Next, slides were incubated with primary antibodies in 5% w/v BSA in PBS overnight at 4°C. Antibodies used were: IFI207-A764 (1:1000),

HA-Alexa594 (1:800, Invitrogen #21288), αFlag (1:1000, Merck #F1804), S5p-RNA pol II (1:1000, Abcam # ab5131), S2p-RNA pol II (1:1000 Abcam #ab5095) and nonspecific rabbit IgG (1-2μg/ml, Sigma #NI01). The next day, cells were washed with PBS and, where required, incubated with secondary αR-Alexa488 (1:800, BioLegend #406416) or αM-Alexa647 (1:800, BioLegend #123122) antibody in 5% (w/v) BSA in PBS for 2 h in darkness at room temperature. After washing, coverslips were mounted with the use of MOWIOL 4-88 (Merck) containing 1 μg/ml DAPI (Merck). Multiple FOVs of each coverslip were taken with the Leica SP8 confocal microscope and images were edited using Laica Application Suite X v. 3.7.4 software.

Flow cytometry

Spleens isolated from the C57BL/6 mice were mashed through the 100 μm cell strainer (OMNILAB) and red blood cells were lysed in Red Blood Cell lysis solution (Miltenyi Biotec) following manufacturers recommended protocol. Cells were then counted and $1x10^5$ of cells from the mixed splenocyte population were centrifuged and stored in -80°C. The rest of the splenocytes were incubated with FC block (BioLegend #101302) at 1/200 dilution in FACS buffer (PBS, 2% v/v FCS, 2 mM EDTA) for 10 min at 4°C. Next, splenocytes were stained with αF4/80-PE (TONBO Biosciences #50-4801), αCD11c-APC (TONBO Biosciences #20-0114), αTCRβ-BV605 (BioLegend #109241) and αCD19-FITC (BioLegend #152404) at 1/100 dilution in FACS buffer for 20-30 min at 4°C. Cells were then washed with FACS buffer and sorted into single stained populations using the FACSAria Fusion (BD Biosciences). $1x10^5$ cells from each single stained splenocyte subpopulation were centrifuged and stored in -80°C until further processing for RNA isolation and RT-qPCR analysis.

Generation and use of *Ifi207*$^{-/-}$ mice

C57BL/6J-Ifi207^{em1Wor} mice (*Ifi207*$^{-/-}$) were generated at UMass Chan Medical School on C57BL/6J background using CRISPR/Cas9 technology. A total of four sgRNA sequences were used: Alcds1gR198r (AGTTCACCCAATCCAGCATCGGG), Alcds1gR199r (CAGTTCACCCAATCCAGCATCGG), Alcds2gR151f (AAGAGACTTCCACAGCTCAGGGG) and Alcds2gR197r (CTCTTTCAGATGTT AGCATGTGG). sgRNAs targeting *Ifi207* coding sequence together with Cas9 mRNA were injected into the B6/J embryos to make Crispr KO mice. PCR genotyping selected CRISPR edited mice were back bred to B6/J for at least 2 rounds to confirm germline transmission. Mice were then rederived from embryos at Comparative Medicine transgenics unit at Trinity Biomedical Sciences Institute (TBSI), Trinity College Dublin. The mice were bred and housed at the TBSI Comparative Medicine Unit and Queens University Belfast.

To genotype *Ifi207*$^{-/-}$ mouse ear punches were dissolved by boiling for 40 min at 95°C in 0.05 M NaOH followed by neutralisation with addition of 1 M TRIS pH 8. Samples were then used for PCR using GoTaq DNA Polymerase (Promega). Two separate PCR reactions were performed for each sample Genotyping PCR primer sequences can be found in Table S2. PCR1 (primers gF1 and gR1) resulted in a band of around 1 kbp detectable in WT but not in the *Ifi207*$^{-/-}$ sample, PCR2 (primers gF2 and gR2) resulted in a 1.65 kbp product detected in WT and a 0.55 kbp product detected in *Ifi207*$^{-/-}$ samples and allowed for identification of heterozygous animals.

Experimental autoimmune encephalomyelitis (EAE)

C57BL/6 (WT) and *Ifi207*$^{-/-}$ female mice were immunized subcutaneously with 100 μg of myelin oligodendrocyte glycoprotein$_{35-55}$ (MOG_{35-55}, GenScript) peptide emulsified 1 in 2 in complete Freund's adjuvant (CFA; Chondrex) on day 0. Mice were then injected intraperitoneally with 250 ng of pertussis toxin (PT, Kaketsucken) on day 0 and 2. Disease severity was assessed up to twice daily depending on percentage weight change and recorded clinical scores. Clinical scores followed a previously published scale.[42] At day 17 (or earlier if clinical scores had exceeded 4 and/or weight loss >20% in comparison to the weight of the animal on day 0), mice were humanely euthanized in compliance with the Irish HPRA. Brains of mice were recovered following cardiac perfusion with PBS and placed in 1ml of TRIzol (Ambion). Tissues were homogenised using a TissueLyser II (Qiagen) tissue homogeniser and RNA was isolated following the manufacturer's protocol. The cDNA was then generated with random hexamers (IDT) using M-MLV reverse transcriptase (MyBio) according to the manufacturer's instructions and gene expression was measured by RT-qPCR.

Intranasal infection of mice with bacteria

K. pneumoniae infections were performed as previously described.[61] Briefly, 8- to 12-week-old wild type (WT) C57BL/6J and *Ifi207*$^{-/-}$ from both sexes were infected intranasally with ~3×10^5 CFU of *K. pneumoniae* (Kp52145) in 30 μl PBS. Mice were also challenged intranasally with $1 x10^8$ CFU *S. aureus* (USA300 LAC) in 20 μl PBS. Non-infected mice were mock infected with sterile PBS only. The number of mice per group are indicated in the figure legends. Mice were sacrificed 24h post infection. For qPCR analysis, lung samples from infected and uninfected control mice were immersed in 1 ml of RNA stabilisation solution (50% (w/v) ammonium sulphate, 2.9% (v/v) 0.5 M ethylenediaminetetraacetic acid, 1.8% (v/v) 1 M sodium citrate) on ice and then stored at 4°C for at least 24 h prior to RNA extraction. Samples were homogenized in 1 ml ice-cold TRIzol using a VDI 12 tissue homogenizer (VWR) or TissueLyser II (Qiagen). RNA was extracted according to the manufacturer's instructions and cDNA was generated by reverse transcription of 1μg of total RNA using M-MLV reverse transcriptase (Invitrogen) and random primers (Invitrogen). RT-qPCR analysis was undertaken as described below. For bacterial quantification, lung samples were immersed in 1 ml sterile PBS on ice and processed for quantitative bacterial culture immediately. Samples were homogenised with a Precellys Evolution tissue homogenizer (Bertin Instruments) or TissueLyser II. Homogenates were serially diluted in sterile PBS and plated onto *Salmonella-Shigella* agar (Sigma) for *K. pneumoniae* or TSA plates (Fisher) for *S. aureus*. The colonies were enumerated after overnight incubation at 37°C. Data were expressed as CFUs per gram of tissue (*K. pneumoniae*) or CFU/ml (*S. aureus*).

Bioinformatics

Phylogenetic comparison of mouse PYHIN family was performed using tools available at Ensembl genome browser (https://www.ensembl.org/index.html). Amino acid sequence alignments were performed using Clustal Omega software (v1.2.4) (https://www.ebi.ac.uk/Tools/msa/clustalo/). ShRNA hairpin sequences were designed with the use of Hairpin Design online software at Genetic Perturbation Platform of Broad Institute (https://portals.broadinstitute.org/gpp/public/).

QUANTIFICATION AND STATISTICAL ANALYSIS

All data were analysed with GraphPad Prism 9 for Windows software. Data are presented as mean ± SEM or SD as specified in the figures. Details of specific statistical tests used (Student's t test, one-way or 2-way Anova, Mann-Whitney test) are described in figure legends and p values of <0.05 were considered as statistically significant. Quantification of microscope images was performed using ImageJ 1.53k software. IFI207 nuclear expression was measured as mean grey intensity within the cell nuclei as defined by DAPI staining. Colocalisation between RNA pol II and IFI207 was measured by quantifying the area of colocalization observed as yellow in relation to the area of IFI207 expression in the cell nucleus and calculated as % of colocalization. For co-localisation of IFI207 and IRF7/IRF7-4D, numbers of cells expressing both proteins and showing colocalisation or no-colocalisation from multiple FOVs were counted and calculated as % of total cells expressing both proteins.

Data availability

All data generated or analyzed during this study are included within this article.